



UNIVERSIDADE D
COIMBRA

Beatriz Fidalgo Gonçalves Pereira Rito

**IMPACT OF GENOMIC BIOPROSPECTING ON THE
OPTIMIZATION OF METALS OBTAINING
PROCESSES IN A CIRCULAR ECONOMY
PERSPECTIVE**

**Dissertação no âmbito do Mestrado em Bioquímica orientada pela Professora
Doutora Paula Maria de Melim Vasconcelos de Vitorino Morais e apresentada ao
Departamento de Ciências da Vida da Faculdade de Ciências e Tecnologia da
Universidade de Coimbra**

Junho de 2020

Departamento de Ciências da Vida da Faculdade de Ciências e Tecnologia da
Universidade de Coimbra

Impact of genomic bioprospecting on the optimization of metals obtaining processes in a circular economy perspective

Beatriz Fidalgo Gonçalves Pereira Rito

Dissertação no âmbito do Mestrado em Bioquímica orientada pela Professora Doutora Paula Maria de Melim Vasconcelos de Vitorino Morais e apresentada ao Departamento de Ciências da Vida da Faculdade de Ciências e Tecnologia da Universidade de Coimbra

Junho de 2020



UNIVERSIDADE D
COIMBRA

Acknowledgments

First of all, I would like to thank to my master thesis supervisor, Professor Doctor Paula Morais for the opportunity to develop this work, all the patience, support and guidance, and for always teach me the best way.

A special thank you to my dear counsellor, colleague and friend Carina Coimbra for always being present and by my side, for always leading me on the right path and for being sincere, honest and friendly.

To my dear Joana Caldeira, a special thank for helping and encourage me, for giving me the right advices and for becoming a great friend.

To Pedro Farias, I appreciate your concern, valid suggestions and opinions that helped me to complete my work; and thank you for also becoming a friend.

To all the colleagues from the Microbiology Laboratory, it was a pleasure to learn with all and thank you for the support, concern and companionship during this year.

To all my friends, thank you for the companionship, concern for my well being and for being the best friends I could have, especially Bárbara Carvalho.

A special thank you to my family, namely my parents and my grandmother, for always being present, for always trust me and in my decisions and for never doubting my abilities.

Finally, to Daniel Santos, a special thank you for being my partner in life, for supporting me and for all your love.

To all, thank you so much.

Index of contents

Acknowledgments	2
Index of contents	3
Index of Figures and Tables	6
Abbreviations and acronyms	9
Abstract	10
Resumo	11
Introduction	12
1. Circular economy	12
2. Metals as raw materials and their importance	14
3. Metal mining exploration and mining wastes	15
4. Microorganisms and their biological processes involving metals	15
5. Bioremediation	17
6. Bioinformatic approach in the genome bioprospecting	18
7. Bioleaching as bioremediation processes.....	18
8. Tungsten	20
8.1. Tungsten in mine exploitation: Panasqueira mine, Portugal.....	20
8.2. Tungsten vs Molybdenum	21
9. Tungsten utilization in bacterial biological systems	22
9.1. Tungstoenzymes	23
10. ABC type transporters	23
10.1. TupABC	25
10.2. WtpABC	25
10.3. ModABC.....	25
11. Recent studies about tungsten	25
Objectives	26
Materials and Methods	27
1. Selected strains	27
1.1. DNA extraction	27
2. Genomic analysis	27
2.1. Phylogenetic tree construction	27
2.2. Bioinformatic screening of tungsten/molybdenum genes coding for transporter systems and other genes responsible for metal mobilization.....	28
3. Detection of specific genes by polymerase chain reaction (PCR) amplification	28
3.1. Screening of modA genes from ModABC transporter system.....	28
3.2. Evaluate modA genes neighborhood on B. simplex 10w-16b	31
3.3. Sequencing and gene sequencing analysis	33
4. Minimum Inhibitory Concentration (MIC) assay	33
5. Tungsten and molybdenum bacterial accumulation assays.....	33
5.1. Growth curve in the presence of metals	34
5.2. Uptake of tungsten and molybdenum during growth.....	34
5.3. Tungsten and Molybdenum uptake competition assay	35
5.4. Bacterial cells metal contents.....	35
5.4.1. Cell digestion by acid lysis	35
5.4.2. Protein quantification through Bradford Method	35

5.4.3. Tungsten and molybdenum measurements	36
5.5. Protein expression analysis	36
5.5.1. Cell lysis	36
5.5.2. SDS-PAGE and sample preparation	36
6. Bacterial bioleaching assays	37
6.1. Monitoring pH variation during bioleaching assay with two different culture media	37
6.2. Tungsten bioleaching determination	37
6.2.1. The impact of a physical barrier during tungsten bioleaching assays	38
6.3. Bioleaching samples treatment	38
7. Confirmation of bioleaching capacity of a selected strain in Lab-scale lysimeters	39
Results	40
1. Genomic Analysis	40
1.1. Phylogenetic tree construction	40
1.2. Bioinformatic screening of tungsten/molybdenum genes coding transporter systems and searching for other genes of metals mobilization	45
2. Detection of specific genes by polymerase chain reaction (PCR) amplification	47
2.1. Screening of modA genes from the ModABC transporter system	47
3. Characterization of the strains as resistant to tungsten and molybdenum	51
4. Characterization of both strains as accumulators	53
4.1. Tungsten and molybdenum accumulation competition assay	56
5. Analysis of protein expression in the absence and presence of tungsten and molybdenum	58
6. Characterization of each strain regarding their capability to bioleach	59
6.1. Bioleaching's culture media determination assay	59
6.2. Bioleaching assay with wolframite or with Panasqueira mine tailings	60
6.3. Bioleaching assay using physical barrier (filter paper)	63
7. Preliminary results of bioleaching capacity of a selected strain in Lab-scale lysimeters	64
Discussion	68
Conclusions	72
References	74
Annexes	78
1. Culture media	78
1.1. Luria-Bertani (LB) medium	78
1.2. Mody-Bam-SM (MBM) medium	78
1.3. Reasoner's 2A broth (R2A) medium	78
2. Solutions and Reagents	79
2.1. Stock solution of Glucose 50%	79
2.2. Stock solution of molybdenum, 1 Molar (M)	79
2.3. Stock solution of tungsten, 1M	79
2.4. Nitric Acid (HNO ₃) solution 10%	79
2.5. Lysozyme solution	79
2.6. Phosphate Buffered Solution (PBS) solution	80
2.7. 1.5M Tris-HCl, pH 8.8	80
2.8. 0.5M Tris-HCl, pH 6.8	80
2.9. Dye solution	80
2.10. Bleach solution	80
2.11. Stock solution of Tris-acetate (TAE) 50x	81

2.12. TAE 1x	81
2.13. Stock solution of Electrode (Running) Buffer 5x (SDS-PAGE)	81
2.14. Electrode Buffer 1x.....	81
3. Agarose gel 1% weight/volume (w/v).....	81

Index of Figures and Tables

Figure 1 – Circular Economy: its dynamics, workflows and concepts it encompasses (Adapted from Mathieux, F., et al. 2017).....	12
Figure 2 – Current contribution of recycling to meet EU demand of CRMs: end-of-life recycling Input Rate (EOL-RIR) versus the CRMs (Adapted from (Mathieux, F., et al. 2017) first Source: JRC elaboration based on (Deloitte Sustainability, 2015) and (Deloitte Sustainability et al. 2017)).....	13
Table 1. List of the 27 Critical Raw Materials determined and published by European Commission in 2017.....	14
Figure 3. Bacterial key roles in biosphere by interactions with metals: summarization of mobilization and immobilization processes (Adapted from Rana, S., et al. 2020)	16
Figure 4. Schematic and representative figure of a lab-scale lysimeter with some examples of possible analysis and samples collections. (Adapted from Grossule, V., et al. 2020)	19
Table 2. Atomic and physical properties of molybdenum and tungsten - commonalities and differences (Adapted from Presta, L., et al. 2015).....	22
Figure 5. Schematic drawing of a generic ABC transporter.. The soluble, periplasmic A-protein scavenges the oxyanion and then binds to the membrane complex, which consists of a pair of translocating, transmembrane B-subunits bound to a cytoplasmic pair of C-subunits with ATPase activity (Adapted from Hagen, W., et al. 2011).....	24
Figure 6. Bacterial oxyanion transporters. A: molybdate transporters; B: tungstate transporters; C: tungstate and molybdate transporters (Adapted from Barajas, E.A., et al. 2011).....	24
Table 3. Forward and reverse specific and degenerated primers sequence designed for amplification of modA gene from B. simplex 10w-16b and C. cellasea 10w-11.....	29
Table 4. Composition of PCR for amplification of modA gene from both bacterial strains.	29
Table 5. Detailed PCR programs with specific primers.	30
Table 6. Detailed PCR programs with degenerated primers.	30
Table 7. Forward and reverse specific primers sequence designed for amplification of hypothetical protein 1 and hypothetical protein 2 from B. simplex 10w-16b.....	31
Table 8. Detailed PCR programs with specific primers for hypothetical protein 1 and hypothetical protein 2 separately on B. simplex 10w-16b.	32
Table 9. Detailed PCR programs with specific primers for half of modA gene and both hypotheticals on B. simplex 10w-16b.	32
Figure 7. Example of an Erlenmeyer with 1g of Panasqueira mine tailings and a paper filter acting as a physical membrane between the bacterial cells and the mine tailings.	38
Figure 8. B. simplex strain B1. S5. 4.2 10w-16b phylogenetic tree.....	41
Figure 9. C. cellasea strain B2. S3. 2.2 10w-11 phylogenetic tree.	43
Table 10. Search by name and function of previously identified W resistant genes and transporters on B. simplex and C. cellasea nearest strains genomes.....	45
Table 11. Search by Blast against genome of previously identified W resistant genes and transporters on B. simplex and C. cellasea nearest strains genomes.	46
Figure 10. Result for searching by function and by Blast against the nearest B. simplex (A) and C. cellasea (B) strain's genomes available on the database. Gene's neighborhood available on JGI IMG/M genomes.....	47
Figure 11. (A) PCR of B. simplex s 10w-16b with specific primers on a 1% agarose electrophoresis gel in TAE 1x, stained with ethidium bromide: well 1- strain 10w-16b; well 2- strain 10w-16b duplicated; well 3- negative control; M- 4µl of NZYTech DNA Ladder III. (B) PCR of C. cellasea 10w-11 with specific primers on a 1% agarose electrophoresis gel in TAE 1x, stained with ethidium bromide: M- 4µl of NZYTech DNA Ladder III; well 1- negative	

control ; well 2- strain 10w-11; well 3 -strain 10w-11 duplicated.....	48
Figure 12. PCR of <i>C. cellasea</i> 10w-11 with degenerated primers on a 1% agarose electrophoresis gel in TAE 1x, stained with ethidium bromide: M- 4µl of NZYTech DNA Ladder III; well 2- strain 10w-11; well 3-strain 10w-11 duplicated; well 4 - negative control.....	49
Figure 13. PCR of <i>B. simplex</i> 10w-16b with specific primers for hypothetical protein 1 and 2 separately on a 1% agarose electrophoresis gel in TAE 1x, stained with ethidium bromide: well 1- strain 10w-16b primers hip1FeR; well 2- strain 10w-16b duplicated primers hip1FeR; well 3- negative control ; well 4- strain 10w-16b primers hip2FeR; well 5- strain 10w-16b duplicated primers hip2FeR ; well 6- negative control ; M- 4µl of NZYTech DNA Ladder III.....	49
Figure 14. PCR of <i>B. simplex</i> 10w-16b with specific primers for hypothetical protein 1 and 2 together on a 1% agarose electrophoresis gel in TAE 1x, stained with ethidium bromide: well 1- strain 10w-16b; well 2- negative control; M- 4µl of NZYTech DNA Ladder III.....	50
Figure 15. PCR of <i>B. simplex</i> 10w-16b with specific primers for half of modA gene and hypothetical protein 2 on a 1% agarose electrophoresis gel in TAE 1x, stained with ethidium bromide: well 1- strain 10w-16b; well 2- strain 10w-16b duplicated; and well 3- negative control. M- 4µl of NZYTech DNA Ladder III.....	51
Table 12. MIC results of the two selected strains, isolated from Panasqueira Mine, at different concentration of W after 3 and 5 days of incubation. +: grow, - does not grow, +/- doesn't grow very well.....	52
Table 13. MIC results of both selected strains, isolated from Panasqueira Mine, at different concentration of Mo after 3 and 5 days of incubation. +: grow, - doesn't grow, +/- doesn't grow very well.....	52
Figure 16. Growth curves of <i>B. simplex</i> 10w-16b (A) and <i>C. cellasea</i> 10w-11 (B) in the absence and presence of W (A1 and B1) and Mo (A2 and B2) both at concentrations of 1mM and 5mM.....	53
Table 14. Values of specific growth rate from growth curves of both strains tested, at different concentration of tungsten and molybdenum.....	54
Figure 17. <i>B. simplex</i> 10w-16b (A) and <i>C. cellasea</i> 10w-11 (B) uptake results for W(A1) and (B1) and Mo (A2) and (B2) at two different concentrations: 1mM and 5mM.....	55
Figure 18. Uptake competition assay for <i>B. simplex</i> 10w-16b where W was the competitor metal and the three experimental conditions were: i) 5mM of Mo and 0mM of W; ii) 5mM of Mo and 5mM of W; and iii) 5mM of Mo and 10mM of W. Cells were recovered at the middle of the exponential phase of the growth curve.....	56
Figure 19. Uptake competition assay for <i>C. cellasea</i> 10w-11: (A) W was the competitor metal and the three experimental conditions were: i) 5mM of Mo and 0mM of W; ii) 5mM of Mo and 5mM of W; and iii) 5mM of Mo and 10mM of W. (B) Mo was the competitor metal and the three experimental conditions were: i) 5mM of W and 0mM of Mo; ii) 5mM of W and 5mM of Mo; and iii) 5mM of W and 10mM of Mo. Cells were recovered at the end of the exponential phase of the growth curve.....	57
Figure 20. (A) - Results of electrophoresis SDS-PAGE (12%) of the protein profile of <i>B. simplex</i> 10w-16b growth with W and Mo at 1mM and 5mM. well 1- strain 10w-16b, well 2- strain 10w-16b with 1mM W, well 3 - strain 10w-16b with 5mM W, well 4 - strain 10w-16b with 1mM Mo and well 5 - strain 10w-16b with 5mM Mo. (B) - Results of electrophoresis SDS-PAGE (12%) of the protein profile of <i>C. cellasea</i> 10w-11 growth with W and Mo at 1mM and 5mM. well 6- strain 10w-11, well 7 - strain 10w-11 with 1mM W, well 8- strain 10w-11 with 5mM W, well 9 - strain 10w-11 with 1mM Mo, and well 10 - strain 10w-11 with 5mM Mo.....	58
Table 15. R2A and MBM culture medium's pH variation during 15 days in a leaching assay with both selected strains and Panasqueira mine tailings.....	59
Figure 21. ICP-MS results of W uptake during bioleaching assay for <i>B. simplex</i> 10w-16b (A) and <i>C. cellasea</i> 10w-11 (B), with wolframite (A1 and B1) and Panasqueira mine tailings (A2 and B2). The W mobilized to the medium in ppm is also shown in line on the right y axis on the graphs.....	60
Table 16. W mobilized to the medium and it respective percentage for <i>B. simplex</i> strain 10w-16b and <i>C. cellasea</i> strain 10w-11 with wolframite concentrated and Panasqueira mine tailings.....	62
Figure 22. Bioleaching values of other metals besides W like Zn, Si and Cu, during bioleaching assay with <i>C. cellasea</i> 10w-11 and Panasqueira mine tailings.....	63
Table 17. W mobilized to the medium and it respective percentage for <i>B. simplex</i> strain 10w-16b and <i>C. cellasea</i> strain	

10w-11 with wolframite concentrated and Panasqueira mine tailings during bioleaching assay with a physical barrier (paper filter).....	64
Figure 23. Lab-scale lysimeters composed by two columns, both filled with Panasqueira mine tailings and MBM medium.	65
Table 18. pH variation during the lab-scale lysimeters bioleaching assay measured in flushing samples (F#) and in suction cup samples (SC#).....	66
Table 19. ICP-MS results of W mobilized to the medium in ppb determined in percolation water and water pore samples during lab-scale lysimeters bioleaching assay.	66
Table 20. ICP-MS results of Se mobilized to the medium in ppm determined in percolation water and water pore samples during lab-scale lysimeters bioleaching assay.	67

Abbreviations and acronyms

°C — degrees Celsius	mg.mL ⁻¹ — milligram per milliliter
% — percentage	mL — milliliter
µm — micrometer	mm — millimeter
µL — microliter	mM — millimolar
µM — micromolar	M — molar
µg.µL ⁻¹ — microgram per microliter	MBM — Mody-Bam-SM
µg.mL ⁻¹ — microgram per milliliter	Mo — molybdenum
µg.mg ⁻¹ — microgram per miligram	nm — nanometers
µ — specific growth rate	NaCl — sodium chloride
bp — base pairs	NaOH — sodium hydroxide
BSA — Bovine Serum Albumine	Na ₂ MoO ₄ ·2H ₂ O — sodium molybdate dihydrate
CRMs — Critical Raw Materials	Na ₂ WO ₄ ·2H ₂ O — sodium tungstate dehydrate
dNTPs — deoxynucleoside triphosphates	OD — optical density
g — gram	pH — -log[H ⁺]
h — hours	PBS — Phosphate Buffered Saline
HNO ₃ — nitric acid	PCR — polymerase chain reaction
ICP-MS — Inductively Coupled Plasma Mass Spectrometry	R2A — Reasoner's 2A
L — liter	rpm — rotation per minute
LB — Luria-Bertani	sec — seconds
MIC — Minimum Inhibitory Concentrations	TAE — tris-acetate
min — minutes	W — tungsten
mg — milligram	

Abstract

Tungsten (W) is a valuable metal with considerable industrial and economic importance with a high supply risk. Therefore, the development of effective and new methods for W recovery is essential to ensure a sustainable supply of this metal. Portugal has one of the largest mines with W, Panasqueira mines, localized in Barroca Grande, generating residues resulting from mine exploration that have been discarded in two tailing basins, being an environmental concern. An in-depth understanding of the Panasqueira mine tailings microbiome and its metabolic capabilities allows the management of tailing disposal sites and the maximization of their utilization as a secondary source in a circular economy perspective.

In this study, two bacterial strains isolated from Panasqueira mine tailings, *Bacillus simplex* 10w-16b strain and *Cellulomonas cellasea* 10w-11 strain were screened for the presence of tungsten/molybdenum transport systems by genome bioprospecting, being identified a *modA* gene in *B. simplex* 10w-16b. The strains were able to grow in the presence of high tungsten and molybdenum concentrations, 100mM of both metals for *B. simplex* 10w-16b and 50mM of W and 20mM of Mo for *C. cellasea* 10w-11. Moreover, strain 10w-11 was able to accumulate up to 60 µg W/mg protein and strain 10w-16b was capable of uptake 2 µg of Mo/mg of protein. Competition uptake assay shown that *B. simplex* 10w-16b has a selectivity to accumulate Mo instead of W. On the other hand, the other strain shown a high selectivity for W.

Biorecovery capability was tested and *C. cellasea* 10w-11 was capable of mobilize to the medium not only W (1.12%) but also other metals that exist in Panasqueira mine tailings, namely Zinc (Zn), Silica (Si) and Copper (Cu).

Biorecovery assays performed with a membrane filter as a physical separation between bacterial cells and the wolframite or mine tailings showed that cells can mobilize metals directly from solid ore being required a physical contact between them.

Bioaugmentation and biostimulation of the Panasqueira mine tailing in lab-scale lysimeters resulted in the mobilization of W at ppb level and mobilization of Se at ppm level.

This study was an important step in the optimization of metals obtaining processes following a circular economy perceptive and in the management of tailings as a secondary sources of W.

Keywords: Tungsten, Molybdenum, genomic bioprospecting, ModABC transport system and biorecovery

Resumo

Tungsténio (W) é um metal valioso com considerável importância a nível económico e industrial com elevado risco de fornecimento. Portanto, o desenvolvimento de novas metodologias eficazes na recuperação de W é essencial para garantir um fornecimento sustentável deste metal. Portugal tem uma das maiores minas de W, localizadas na Barroca Grande, que gera resíduos resultantes da exploração mineira que têm sido descartados em duas bacias de rejeitados, sendo um foco de preocupação ambiental. A compreensão aprofundada do microbioma dos resíduos da mina da Panasqueira e as suas capacidades metabólicas permite uma melhor gestão dos locais de descarte dos rejeitados mineiros bem como a maximização da sua utilização como fontes secundárias para a obtenção de metal, numa perspetiva de economia circular.

No presente trabalho, nas estirpes bacterianas isoladas a partir dos resíduos da mina da Panasqueira, *Bacillus simplex* 10w-16b e *Cellulomonas cellasea* 10w-11 foi determinada a presença de sistemas de transporte de tungsténio/molibdénio por bioprospeção genómica, tendo sido identificado um gene *modA* na estirpe *B. simplex* 10w-16b. As estirpes foram capazes de crescer na presença de elevadas concentrações de tungsténio e molibdénio, 100mM de ambos os metais no caso da *B. simplex* 10w-16b e 50mM de W e 20mM de Mo para a *C. cellasea* 10w-11. Além disso, a estirpe 10w-11 foi capaz de acumular até 60 µg W/mg proteína e a estirpe 10w-16b acumulou 2 µg of Mo/mg of proteína. Os ensaios de competição de acumulação mostraram que *B. simplex* 10w-16b apresenta maior seletividade para bioacumular Mo em vez que W. Por outro lado, a outra estirpe apresentou elevada seletividade para W.

A capacidade de biolixiviação foi testada e *C. cellasea* 10w-11 foi capaz de mobilizar para o meio não só W (1.12%) mas também outros metais que existem nos resíduos da mina da Panasqueira, nomeadamente Zinco (Zn), Sílica (Si) e Cobre (Cu).

Os ensaios de lixiviação que foram realizados com a utilização de um filtro membranas atuando como separação física entre as células bacterianas e a volframite ou os resíduos mineiros, mostraram que as células conseguem mobilizar o metal diretamente a partir do minério sólido, sendo necessário um contacto físico direto.

A bioaugmentação e bioestimulação nos sedimentos da mina da Panasqueira em sistema de colunas à escala laboratorial resultou na mobilização de W em ppb e na mobilização de Se em ppm.

O presente trabalho foi um importante passo na otimização de processos de obtenção de metais numa perspetiva de economia circular e na gestão de resíduos mineiros como fonte secundária para a obtenção de W.

Palavras-chave: Tungsténio, Molibdénio, bioprospeção genómica, sistema de transporte ModABC e biolixiviação,

Introduction

1. Circular economy

Sustainability has been a main keystone in the political agenda as well as the global research (D'Amato, D., *et al.* 2017), once there is limited availability of many natural sources (Fellner, J., *et al.* 2017). So, it is necessary to develop environmentally-friendly methodologies and technologies for the recovery of metals in ores by minimizing resource extraction, maximizing reuse, increasing efficiency and developing new business models. All waste is used as a secondary raw material, in other words, through a circular economy perspective (Cortez, H., *et al.* 2010; Wang, X., *et al.* 2019).

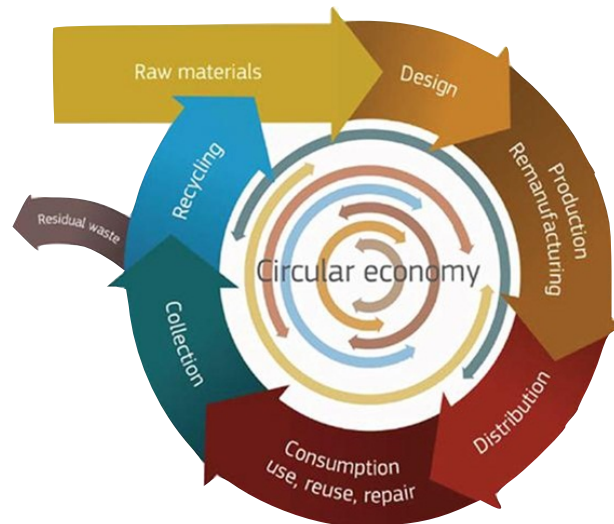


Figure 1 – Circular Economy: its dynamics, workflows and concepts it encompasses (Adapted from Mathieux, F., *et al.* 2017).

The circular economy, as illustrated in **Figure 1**, is a strategic concept based on the reduction, reuse, recovery and recycling of materials and energy. It is seen as a key element in promoting decoupling between economic growth and increased consumption of resources (Eco.nomia 2020; D'Amato, D., *et al.* 2017).

Recycling is an important process to obtain secondary raw materials (SRMs). It can contribute to a “greener” supply of raw materials and advancing through a circular economy in wastes management. Several CRMs have high recycling potential. However, despite the government's support to move towards a circular economy, the end-of-life recycling input rate (EOL-RIR, measurement of how much the total material input into the production system results from recycled waste) is commonly low (Mathieux, F., *et al.* 2017). Yet, a few critical raw materials, for instance, vanadium (V), tungsten (W) and cobalt (Co) have a high recycling-input

rate, as presented in **Figure 2**. Such encouraging values can be because since the recovery at the “end of life” is high and once W is mainly used in high-tech equipment, V is in steel alloys and Co is used primarily in batteries, they are well collected at the end-of-life because of the waste legislation (Mathieux, F., *et al.* 2017).

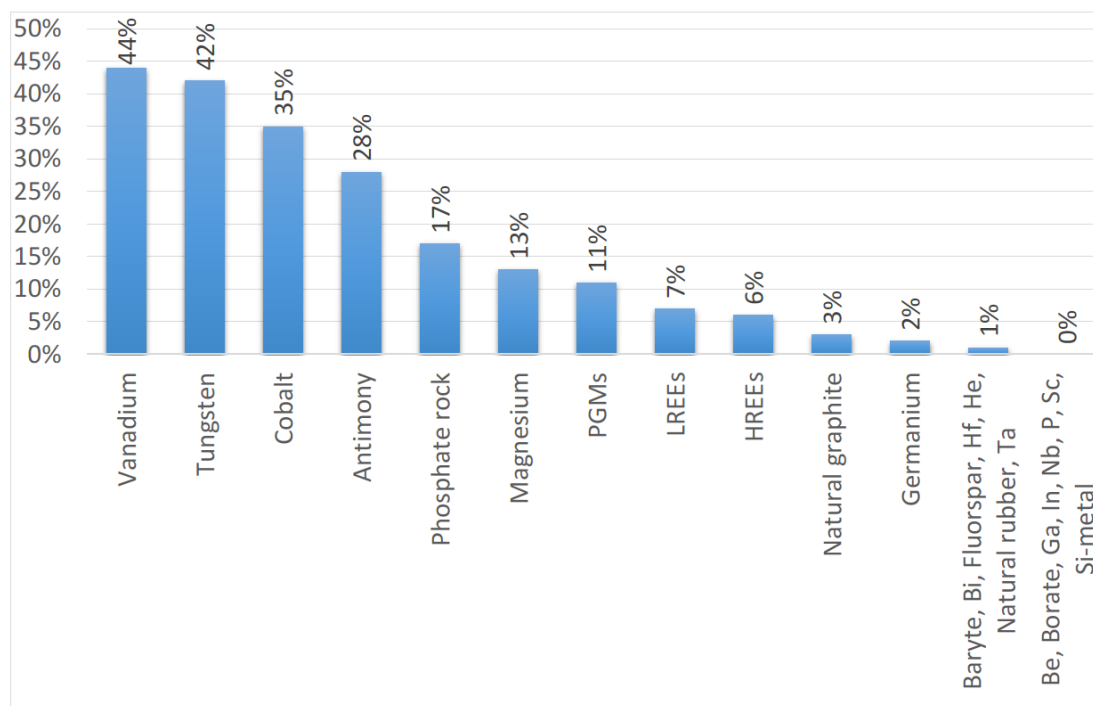


Figure 2 – Current contribution of recycling to meet EU demand of CRMs: end-of-life recycling Input Rate (EOL-RIR) versus the CRMs (Adapted from (Mathieux, F., *et al.* 2017) first Source: JRC elaboration based on (Deloitte Sustainability, 2015) and (Deloitte Sustainability *et al.* 2017)).

It is possible to understand that the circular use of CRMs is depending on several parameters. The circularity is highly influenced by the sectors in which raw materials are inserted. The performance and applicability of recycling methodologies and technologies are depending upon the nature of the waste or end-of-life products where CRMs are incorporated (Mathieux, F., *et al.* 2017). Despite that, it is expected that the application of a circular economy includes benefits by reducing the demand for primary sources of raw materials, reducing environmental issues, lower wastes volume and less landfill space required, creation of a “greener” employments and improvement for economic growth (Fellner, J., *et al.* 2017; Jones, P., *et al.* 2020). Is due to this and based on the “Raw Materials Initiative” project from European Union (EU), that was released an action plan for a circular economy (COM/2015/0614 Circular Economy Package): an EU plan that emphasizes a “transition to a more circular economy, where the value of products, materials and resources is maintained in the economy for as long as possible, and the generation of waste minimized, which is seen as an essential contribution to the EU’s efforts to develop a sustainable, low carbon, resource-efficient and competitive economy” (Fellner, J., *et al.* 2017; European Commission, 2017).

2. Metals as raw materials and their importance

Metals elements can be defined and distinguished from nonmetals and metalloids by their physical properties such as malleability, ability to conduct heat, electrical resistance (directly related to temperature), lustre, among others (Appenroth, K.J., *et al.* 2010). Metals originate from natural sources such as rocks and metalliferous minerals but also anthropogenic inputs like agriculture, metallurgy, waste disposal and mining. They are ubiquitous and exist in diverse forms in the biosphere constituting about 75% of the known elements (Gadd, G.M., *et al.* 2010; Cortez, H., *et al.* 2010). Metals are involved directly or indirectly in biological processes as microbial growth, metabolism and differentiation. They are raw materials once metals are also vital to daily life, infrastructure and industry. European Union created a list of Critical Raw Materials based on the economic importance and the supply risk of the material (Gadd, G.M., *et al.* 2010; European Commission, 2017).

Table 1. List of the 27 Critical Raw Materials determined and published by European Commission in 2017.

Aluminum (Bauxite)	Chromium	Helium	Potash	Tellurium
Antimony	Cobalt	Indium	REEG	Tin
Arsenic	Fluorspar	Lithium	Rhenium	Titanium
Barite	Gallium	Magnesium	Rubidium	Tungsten
Beryllium	Germanium	Manganese	Scandium	Uranium
Bismuth	Graphite (natural)	Niobium	Strontium	Vanadium
Cesium	Hafnium	PGMs	Tantalum	Zirconium

The list of 27 Critical Raw Materials (CRMs) created by European Commission in 2017 is shown in **Table 1**. This list includes a group of metals that need to be secured for sustainable production of key components of various products such as low carbon energy technologies, automobiles, electronic and biomedical devices. This list is subject to a regular review and updated. As a consequence of their importance for the economy, industry, modern technology, environment, and/or their scarce availability, new strategies to obtain these metals are urgently needed (Gadd, G.M., *et al.* 2010; European Commission, 2017; Wang, X., *et al.* 2019).

Raw materials and their applicabilities are crucial for the re-industrialization and for the Europe economy. The increased demand for raw materials over the last centuries is closely and directly relates to the fast industrial growth (Cortez, H., *et al.* 2010; Wang, X., *et al.* 2019) and their exploitation was focused in high grade ore deposits, extracted and treated by conventional

techniques. The metal recovery efficiency of these techniques was low, resulting in a significant amount of discarded tailings dams (Gadd, G.M., *et al.* 2010).

3. Metal mining exploration and mining wastes

Mine tailings are generated from the mechanical and chemical processing of ores. Since the extraction process is less than 100%, a large quantity of non-economic material, containing substantial amounts of metals, is discarded and can eventually mobilize the metals into the environment. Only less than 2% of all extracted metal from the mines corresponds to the economical valuable metal, while the rest is discarded as waste and usually deposited in areas close to the mining operation (Cortez, H., *et al.* 2010). Per year, metal mining exploration generates large volumes of mining waste and, according to the Mining, Minerals, and Sustainable Development Project (MMSD), there are nearly 3500 active mining waste facilities worldwide (Tayebi-Khorami, M., *et al.* 2019). The estimated generation of solid tailings resulting from the primary exploration of mines is about 100 billion tons per year and it can depend on the mass of the valuable element, ranging several times. However, the main concern about mine tailings is their significant pollution generation, not only through air pathways, as dust and gas emissions, but also related to the possibility of leaching into the water (Tayebi-Khorami, M., *et al.* 2019).

There is a growing concern with the environment. One of the biggest challenges is how to deal with the huge amount of mining waste, generated in the mining processes, and the resulting leachates from the mine's environment. The treatment of old abandoned deposits and other secondary resources related to mining activities in the past have attracted increasing interest (Cortez, H., *et al.* 2010; Wang, X., *et al.* 2019). Today, mines still producing residues and tailings and new strategies and approaches have been developed to solve these issues. One promising approach consists in an indepth understanding of the tailings microbiome and its metabolic capabilities, providing this way a direction for the management of tailings disposal sites and maximize their potential as secondary resources (Chung, A.P., *et al.* 2019). Moreover, characterization of autochthonous microorganisms with the potential to be applied in biological processes (further developed in point 4) such as biosolubilization, biomineralization and bioaccumulation, are needed to develop novel strategies for the recovery of metals from mine tailings as part of a circular economy (Chung, A.P., *et al.* 2019).

4. Microorganisms and their biological processes involving metals

Bacteria play important roles in the environmental fate of toxic metals and ores by a variety of biological and physicochemical mechanisms, affecting transformations between insoluble and soluble phases (White, C., *et al.* 1997; Valls, M., *et al.* 2002). Some bacteria demonstrated capacity to resist to metals and metabolize them in soil, water, industrial waste and

mine tailings, and these mechanisms have potential application to the treatment of contaminated materials and the recovery of metal from secondary sources as mines tailings (Anjum, F., *et al.* 2012).

Metals at higher concentration than their basal level in the environment are potentially toxic to microorganisms and the inclusion of metals in its various forms in the environment can induce modifications at the microbial communities level and in their activities and interactions (Bruins, M.R., *et al.* 2000; Hassen, A., *et al.* 1998). This can occur by alterations in the conformational structure of nucleic acids and proteins, by blocking essential functional groups, interference with oxidative phosphorylation and osmotic balance, displacing essentials metals or modifying the active conformations of molecules (Bruins, M.R., *et al.* 2000; Hassen, A., *et al.* 1998). The tolerance to metals and the impact of biological processes on metal contaminations will depend on several factors as the chemical environment, the nature of the contaminated site, the metal bioavailability and its concentration (Hassen, A., *et al.* 1998).

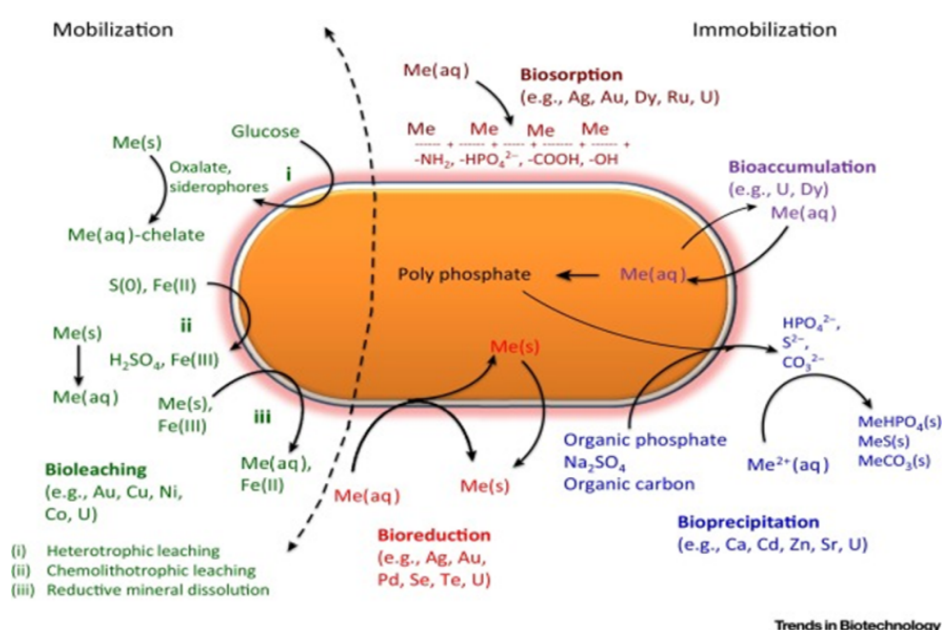


Figure 3. Bacterial key roles in biosphere by interactions with metals: summarization of mobilization and immobilization processes (Adapted from Rana, S., *et al.* 2020).

Bacteria's biological processes can either mobilize or solubilize metals, as illustrated in **Figure 3**, increasing their bioavailability as well as their toxicity potential; or immobilize, reducing their bioavailability (Unz, R.F., *et al.* 1996; Anjum, F., *et al.* 2012; Adams, G.O., *et al.* 2015). Intracellular accumulation, i.e. active bioaccumulation, is an immobilization and energy-driven biological process dependent on active metabolism that normally occurs when a metal is retained by an organism (Anjum, F., *et al.* 2012; Adams, G.O., *et al.* 2015; Coimbra, C., *et al.* 2017). Siderophores are bacterial metabolites with low molecular weight and high affinity to metals excreted by bacteria in the environment near them. Siderophores solubilize metals forming stable compounds (chelation) which are then absorbed into the bacterium. Microorganisms can also contribute to metal immobilization by exopolymers and by precipitation of insoluble

inorganic and organic compounds. Immobilization processes are particularly applicable to removing metals from mobile phases, such as leachates and ground waters (Anjum, F., *et al.* 2012; Adams, G.O., *et al.* 2015). Alternatively, metal mobilization can be carried out by a range of processes like autotrophic (chemolithotrophic) and heterotrophic leaching. Bioleaching processes, consist in microbiological solubilization of metals from solid minerals. Thus, bioleaching is mainly a process based on three mechanisms: i) proton-induced metal solubilization; ii) metal reduction or oxidation (redox modifications); and iii) metals mobilization from solid materials by ligand-induced metal solubilization where ligands can be organic acids such as citric and oxalic acids, resulting in leachates with high content of soluble metal ions potentially hazardous (Gadd, G.M., *et al.* 2010; Cortez, H., *et al.* 2010; Anjum, F., *et al.* 2012).

5. Bioremediation

Conventional techniques to remove metals from a large number of wastes include chemical precipitation, filtration, ion exchange and electrochemical processes (Leong, Y.K., *et al.* 2020). However, these methodologies have high maintenance costs and consequent secondary pollution resulting from the production of toxic compounds. An environmentally friendly and with a low cost-efficiency alternative to the conventional methods is bioremediation of metals using different microorganisms including bacteria, fungi, yeast and even microalgae (Leong, Y.K., *et al.* 2020). So, bioremediation is the application of biological systems to “clean-up” organic and inorganic pollution. Microorganisms are important for the recovery, immobilization, and detoxification of several wastes such as mine tailings potentially hazardous to the environment (White, C., *et al.* 1997; Adams, G.O., *et al.* 2015). This process can function naturally but can also be improved with the addition of several nutrients, electron acceptors, or other factors (Ayangbenro, A.S., *et al.* 2017).

Currently, there is an emerging trend of bioremediation consisting of employing microalgae as biosorbents or bioaccumulators of pollutants according to Leong and colleagues (Leong, Y.K., *et al.* 2020). Bacteria can also be used in remediation processes taking advantage of the capability to resist and metabolize metals of some bacterial strains (Ayangbenro, A.S., *et al.* 2017) and promoting the bioaugmentation of selected bacterial strains with that characteristics (Gadd, G.M., *et al.* 2010; Cortez, H., *et al.* 2010; Adams, G.O., *et al.* 2015). This strategy involves the introduction of autochthonous microorganisms, i.e., isolated from the same environment where are going to be inoculated, to favor their growth in the bacterial community, taking advantage of their metabolic capabilities and interactions. Other alternative that leads to an improvement of biological processes is the biostimulation of indigenous microbial populations just by adding nutrients or electron acceptors/donors or adjusting the pH and redox potential, stimulating the growth of the entire community (Cortez, H., *et al.* 2010). Bioremediation processes, as bioaugmentation and biostimulation, are according with a circular economy perspective and applied in a contaminated mine environment, this kind of processes are a possible solution to promoting the obtention of metals from secondary sources, the mining wastes (Adams, G.O., *et al.* 2015).

6. Bioinformatic approach in the genome bioprospecting

The metabolic functions of the microbiomes and the autochthonous bacterial strain's genome bioprospecting can be performed using a computational approach with bioinformatic tools (Chung, A.P., *et al.* 2019).

Namely in a bioremediation process of bioaugmentation, the most promising autochthonous bacterial strains to bioaugmentate can be predicted through a genomic analysis, using complete genomes available in genomes databases as JGI IMG/M genomes database for further screening for the presence of genes encoding for proteins/transporters of interest (Markowitz, M., *et al.* 2012). Bacterial strains' metabolic pathways can also be inferred in available metabolic pathways databases such as KEGG database or using computational softwares as PICRUSt software (Markowitz, M., *et al.* 2012; Chung, A.P., *et al.* 2019).

Bioinformatics enrichment tools have played a very important and successful role contributing to the gene functional analysis, and the complement of a bioinformatic approach with a molecular biology techniques provides a better understanding of genes and genomes (Huang W., *et al.* 2009).

7. Bioleaching as bioremediation processes

In the field of bioremediation of contaminated sites as mines, bioleaching is a promising emerging “green” technology, because besides being a simple process, it has low energy requirement, needs low capital investment and has reduced environmental impact. The advantages of this capacity of solubilizing make it an effective method for metal extraction, environmental protection as well as waste utilization and reuse (Wang, X., *et al.* 2019; Adams, G., *et al.* 2015). According to the literature, bioleaching processes have already been applied for the extraction of various metals. The extraction of copper (Cu) was demonstrated by Díaz and colleagues (Díaz, J.A., *et al.* 2018) and the extraction of zinc (Zn) by Deveci and colleagues (Deveci, H., *et al.* 2004), referring as well the importance of the pH factor during the bioleaching process. The research work of Li and colleagues (Li, S., *et al.* 2014) was based on nickel (Ni) bioleaching and enforcing the key role of an amino acid (L-Cysteine) in the maintenance of an indicated pH value. Bioleaching has also been applied for the obtention of uranium (U) (Wang, X., *et al.* 2019) and gold (Au) (Egan, J., *et al.* 2016), both showing that metal dissolution increases with the decreasing of the particle size.

These bioleaching capabilities have so practical applications in the recycling of resources from many industrial sectors, especially in mining exploration, and are proving to be a profitable alternative to conventional and traditional mining technology (Wang, X., *et al.* 2019; Adams, G., *et al.* 2015). The leached metals in the leachate can be quantified by Inductively Coupled Plasma Mass Spectrometry (ICP-MS) (Coimbra, C., *et al.* 2019).

There are different kind of reactors setups for bioleaching reactions, namely growth in batch culture or lab scale lysimeters. It is known that there are different parameters that affect the efficiency of bioleaching processes executed by microorganisms from contaminated soils and tailings, including pH, temperature, medium composition, particle size and pulp density (Ayangbenro, A.S., *et al.* 2017; Rasoulnia, P., *et al.* 2020).

In the evaluation and optimization of bioleaching processes, it is known that column tests, with lab-scale lysimeters, are much closer to the real conditions of a particular contaminated site than batch shaking tests. In the last years, several works have been published on the evaluation and analyze of residues/wastes and their reuse (Grathwohl, P., *et al.* 2014). A schematic example of a lab-scale lysimeter is represented in **Figure 4**.

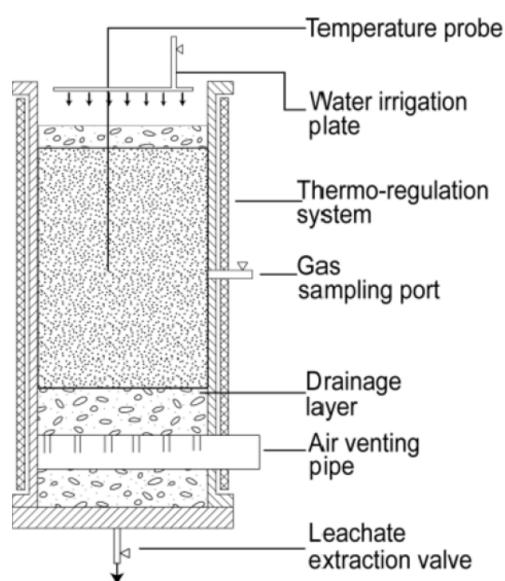


Figure 4. Schematic and representative figure of a lab-scale lysimeter with some examples of possible analysis and samples collections. (Adapted from Grossule, V., *et al.* 2020)

Lab-scale lysimeters can have several dimensions and allows to analyze various parameters, like temperature, gas production or water flux, depending on the solid waste inside the column. Flushing samples can be collected by a leachate extraction valve under the column. Water pore and solid samples can also be collected (Grossule, V., *et al.* 2020). Despite the variety of analyzes it allows and the possibility to compare factors and the advantages towards batch tests, there are some uncertainties regarding equilibration of the percolation water with the solids such as liquid-to-solid ratios and the column equilibration, that might potentially lead to underestimation of contaminant concentrations in the effluent (resultant leachate) (Grathwohl, P., *et al.* 2014; Grossule, V., *et al.* 2020).

8. Tungsten

Tungsten fits in the sixth group of the periodic table along with molybdenum (Mo) and chromium (Cr), belonging to the transition metals block. Tungsten has an atomic number of 74 and the main source of this metal, as well as its most stable oxidation state in aqueous environments, is the oxyanion tungstate (WO_4^{2-}) (Bevers, L.E., *et al.* 2009; Coimbra, C., *et al.* 2017). No element of the third row of transition elements is known to exhibit biological activity in enzymes except for W which is the element with the highest atomic number used by living organisms (Andreesen, J.R., *et al.* 2008). It has been described as being an essential element for some microorganisms belonging to Archaea and Bacteria domains, playing an essential biological role in their life processes being required as a nutrient (Coimbra, C., *et al.* 2019). For other microorganisms, W is a facultative bioelement, i.e. the microorganisms can choose to make biological use of the metal but only where they experience specific environmental limitations. For the remaining microorganisms, this metal is biochemically indifferent, or even a foreign element, once they have not developed mechanisms to incorporate W. This metal can be present in different habitats, such as hot black smokers, sulfide-enriched waters or in environments for mining wolfram extraction and its resulting mine tailings.

Tungsten is found as oxo-rich tungstate minerals (W(VI)), as scheelite (CaWO_4) and wolframite ($(\text{Fe/Mn})\text{WO}_4$), and the more reduced, being very rare, tungstenite (WS_2 (W(IV))) (Godinho, B.R.C., *et al.* 2009). Tungsten can form compounds with valence states from -2 to -6. However, this metal is described to be transported into the bacterial cells in the ionic form of WO_4^{2-} (Coimbra, C., *et al.* 2017).

Tungsten in its pure form has the highest melting point and is considered to be a critical metal. Tungsten is one of the most important metals with high economic importance and high supply risk (Coimbra, C., *et al.* 2017). It is used in many key industries once it is a critical metal essential for the production of the world's technologies based on high-tech economy LCD panels, TV tubes, laser printers and window heating wires. This high-tech industry is at risk due to tungsten's imminent shortages and rising prices. Therefore, it is anticipated that, because of the development of the industrial sectors and a growing global population, the demand for W will continue to increase (Coimbra, C., *et al.* 2017; Coimbra, C., *et al.* 2019). Thus, for ensuring a sustainable supply of W, it is imperative the development of more effective, economically profitable and environmentally friendly technologies for the recovery of this heavy metal from mine tailings.

8.1. Tungsten in mine exploitation: Panasqueira mine, Portugal

Panasqueira mine, localized in Barroca Grande, Portugal, close to the town of Fundão - central Portugal. It is the largest producer of W concentrates in Europe and one of the largest operating tungsten mines in the Market Economy Countries (Godinho, B.R.C., *et al.* 2009;

Gonçalves, A.C.R., *et al.* 2012). The region of the mines is characterized by an average annual rainfall of 1183mm and an annual average temperature of 15.1°C. The area surrounding the mine is composed by a pine forest with no anthropogenic interference and by two tailings basins where all the resulting waste from the mine exploitation are stored (Chung, A.P., *et al.* 2019).

Until now, this Portuguese mine has produced million tons of wastes and residues during its almost 120 years of operation. Some of these residues resulting from mining exploration and ore processing consist in sediments and materials that may have interesting levels of W and other metals, depending on the efficiency of the technologies applied throughout the life span of the mine. All these residues have been discarded in two tailing basins. The first basin was closed in 1985 and the second basin is the nowadays the only one that receives mine tailings. It is known that mine tailings are oligotrophic environments full of toxic metals, becoming a challenging environment for microbial survival. However, despite of the metals' toxicity, a high diversity of microbial communities in mine tailings playing important ecological and biogeochemical roles have been reported (Chung, A.P., *et al.* 2019).

In recent years, some studies have been done to determine the soil and water contamination levels in the surroundings of the Panasqueira mine, as well as the potential of dispersion of the contaminants to bordering areas. Other studies aimed to understand the challenges in the valorization of minerals as a contribution to a circular economy in the Central Region of Portugal. Chung and colleagues (Chung, A.P., *et al.* 2019) had provided an in-depth understanding of the Panasqueira mine tailings microbiome and its metabolic capabilities in order to optimize the management of tailing disposal sites and to maximize their utilization as a secondary source in a circular economy perspective. Despite of significant differences in tailings physicochemical properties, in the mine tailings microbiome were found members of family *Anaerolineacea* and genera *Acinetobacter*, *Bacillus*, *Cellulomonas*, *Pseudomonas*, *Streptococcus* and *Rothia* (Chung, A.P., *et al.* 2019).

8.2. Tungsten vs Molybdenum

As mentioned before, W is in the same periodic table group as Mo, both belonging to the transition metals block. They are chemically analogous elements, and both are relatively scarce in natural environments. Their physical and chemical similar properties are based on equal atomic, ionic radii, coordination characteristics and similar electronegativity (Andreesen, J.R., *et al.* 2008; Presta, L., *et al.* 2015). The commonalities and differences between some W and Mo properties can be seen on **Table 2**.

Table 2. Atomic and physical properties of molybdenum and tungsten - commonalities and differences (Adapted from Presta, L., *et al.* 2015).

	Molybdenum	Tungsten
Atomic number	42, transition metal	74, transition metal
Atomic mass	95.94 g amu	50.9415 amu
Electronic configuration	[Kr]4d5s1	[Ar]3d34s2
Oxidation states	2, 3, 4, 5, 6	5, 3
Density	10.280 kg/m ³	6110 kg/m ³
Covalent radius	145 pm	125 pm
Cristal structure	Body centered cubic	Body centered cubic
Melting point	2896 K	2175 K
Boiling point	4912 K	3682 K
Electronegativity	2.16	1.63
Free energy of solvation	-226.8 kcal mol ⁻¹	-230.1 kcal mol ⁻¹
Covalent solution radii	2.75 Å	2.83 Å

The similarity between these oxyanions can lead to a lack of ability to distinguish them by the biological systems, leading to the toxicity of WO_4^{2-} . However, from a biological perspective, W and Mo provide a range of contrasts. Mo has essential roles in several fundamental biological conversions carried out by various microorganisms. On the other hand, W has been regarded as an antagonist of the biological functions of Mo. Based on the similarities of these two elements, it was considered that the catalytic role of Mo in several enzymes could be provided by replacing Mo with W. However, the chemical properties of these two metals are sufficiently different that biological systems are capable of distinguishing between them, not only at the levels of their uptake and incorporation into enzymes but also in the enzymes' properties, which function with Mo but not with W (Johnson, M.K., *et al.* 1996).

9. Tungsten utilization in bacterial biological systems

Bacteria having enzymes dependent on W or Mo for biological functions need to incorporate them into their cells where it will only show biological activity after being incorporated into cofactors, designated as tungstopterin and molybdopterin, respectively. This incorporation into cofactors allows efficient control of the redox properties of the metal. These cofactors usually have sulfur atoms from three ligands of the metal in concern together with two oxygen atoms. It is well known that cellular uptake of metals from the environment can occur by: i) a selective substrate-specific uptake system with the consumption of energy (ATP) designated

as active transport; and ii) a substrate-non-specific uptake system that uses the chemiosmotic gradient designated as passive transport. Tungsten and Mo are present in enzymes with the catalytic activity of the oxygen atom transfer reactions (Coimbra, C., *et al.* 2017) and both metals are also required for the assembly and function of molybdoenzymes and tungstoenzymes. The last one is considered to be more evolutive ancient than molybdoenzymes (Hagen, W.R., *et al.* 2011).

9.1. Tungstoenzymes

Tungstoenzymes, or W-containing enzymes, can be divided into different categories as the aldehyde oxydoreductases (AORs) and the formate dehydrogenases (FDHs). These enzymes are mostly found in anaerobic prokaryotes, as well as hyperthermophilic archaea: obligatory W-dependent, and have also been identified in aerobic proteobacteria, being present in a wide range of microorganisms (Johnson, M.K., *et al.* 1996).

10. ABC type transporters

ABC-type transporters include transporters systems that allow the active uptake/extrusion of various substrates into the interior/exterior of the cells. W and Mo are two of the metals that are transported by ABC-type transporters. This type of transporters allows bacteria to scavenge WO_4^{2-} and molybdate (MoO_4^{2-}) oxyanions. Is due to their shape, charge and size similarities that both oxyanions may be transported by the same carriers (Barajas, E.A., *et al.* 2011). All these systems are members of the adenosine triphosphate (ATP) ABC-binding cassette transporter family (Hagen, W.R., *et al.* 2011). The organization of these transporters is consisted of three proteins. The “A” protein is responsible for the recognition and binding of the substrate, being located in the space between the cytoplasmatic membrane and the cell wall in Gram-positive bacteria, the outer membrane in Gram-negative bacteria, or the S-layer in the case of Archaea. So, the “A” protein is located, in a general way, in the periplasm on Gram negative bacteria. The “B” protein, that forms a transmembrane pore, allows the substrate to be transported into the cell and the “C” protein with ATP hydrolyzing activity that facilitates the substrate transport, and it is located in the inner surface of the cell membrane (Barajas, E.A., *et al.* 2011; Bevers, L.E., *et al.* 2009). This organization of an ABC-type transporter is schematized in **Figure 5**.

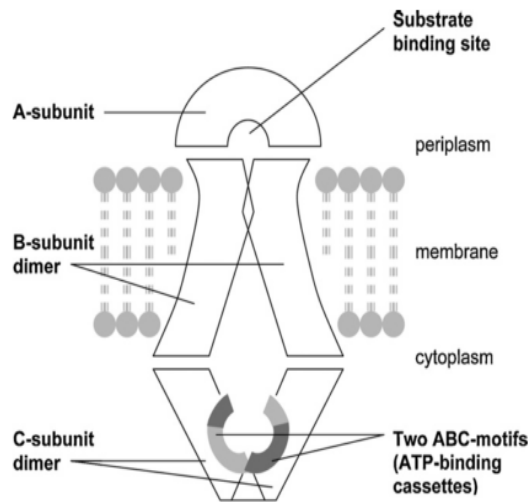


Figure 5. Schematic drawing of a generic ABC transporter. The soluble, periplasmic A-protein scavenges the oxyanion and then binds to the membrane complex, which consists of a pair of translocating, transmembrane B-subunits bound to a cytoplasmic pair of C-subunits with ATPase activity (Adapted from Hagen, W., *et al.* 2011).

According to the literature, W and Mo can be taken into the cells by three known different transporters ABC-type, as illustrated in **Figure 6**.

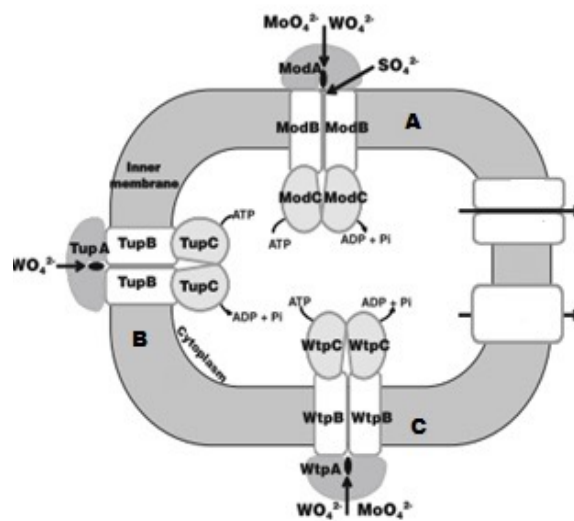


Figure 6. Bacterial oxyanion transporters. **A:** molybdate transporters; **B:** tungstate transporters; **C:** tungstate and molybdate transporters (Adapted from Barajas, E.A., *et al.* 2011).

The tungstate uptake transporter (TupABC) is highly specific for WO_4^{2-} , the W-transport (WtpABC) transports both WO_4^{2-} and MoO_4^{2-} and the molybdate transporter (ModABC) which is highly specific for MoO_4^{2-} can also carry WO_4^{2-} (Bever, L.E., *et al.* 2009; Coimbra, C., *et al.* 2017; Barajas, E.A., *et al.* 2011).

10.1. TupABC

TupABC was identified for the first time in the mesophilic bacterium *Eubacterium acidaminophilum*. TupA is a binding protein, that is highly specific in the case of WO_4^{2-} . With low specificity for bind MoO_4^{2-} , and it does not bind sulfate, chromate, selenite, or phosphate (Bever, L.E., *et al.* 2009; Barajas, E.A., *et al.* 2011).

10.2. WtpABC

WtpABC transporter was discovered in the hyperthermophilic archaean *Pyrococcus furiosus* and it can take up both WO_4^{2-} and MoO_4^{2-} . WtpA has a higher affinity to W than ModA and its affinity for Mo is similar to that of ModA (Barajas, E.A., *et al.* 2011).

10.3. ModABC

The high-affinity ModABC system belongs to the MoO_4^{2-} uptake transporter family, also transporting WO_4^{2-} and sulfate. This ABC transporter has been well characterized in *Escherichia coli* and it is encoded by the *modABC* operon (Bever, L.E., *et al.* 2009; Barajas, E.A., *et al.* 2011).

11. Recent studies about tungsten

In recent studies, Coimbra and colleagues (Coimbra, C., *et al.* 2017) found three different strains from *Sulfitobacter dubius* with the genes' organization in the operon showing to be *tupBCA* instead of *tupABC* or *tupACB*, as presented in the available databases, namely NCBI and Gene Bank. Similar strains belonging to the same species, carrying the same *tup* genetic organization and having high homology among their genes, exhibited distinct profiles and efficiencies for W-uptake. Later, Coimbra and colleagues (Coimbra, C., *et al.* 2019) complete *tup* gene cluster from *Sulfitobacter dubius* NA4 in *E. coli* cells resulting in a high bacterial capacity to accumulate W, also able to accumulate Mo and Cr. This study showed an alternative strategy to recover W from natural environments or anthropogenic W-impacted environments and from lecheates with high amounts of this metal solubilized.

Objectives

The main objective of this work was to characterize two autochthonous strains isolated from Panasqueira mine tailings. This was done to get more information to further allow us to understand the role of the mine tailings microbiome in the W mobilization. Moreover, this work wanted to evaluate the use of the mine tailings as secondary sources of metals to be recovered by bioaugmentation using the two autochthonous strains, and develop a conceptual strategy to reduce the environmental damage of mining wastes.

To fulfill this objective, the first task was to select the most promising bacterial strains isolated from Panasqueira mine's basins, an environment contaminated with metals. In the second task, the presence of metal resistance genes (for example, *tupABC* and *modABC*) in their genomes were screened and analyzed by bioinformatic tools, and further using molecular biology tools. The applicability of these microorganisms, with the target genetic and metabolic characteristics, was studied on third and fourth tasks, for the metal accumulation process in the presence of tungstate, as well as their ability to bioleach ore (W concentrate) and tailings from Panasqueira mine.

In the last chapter, the selected strains' metals bioleaching capability was preliminary explored with lab-scale lysimeters filled with Panasqueira mine tailings as a pilot system of a strategy of metal recovery from secondary sources, using a bioprocess.

Materials and Methods

1. Selected strains

Two bacterial strains namely *Bacillus simplex* strain B1. S5. 4.2 10w-16b and *Cellulomonas cellasea* strain B2. S3. 2.2 10w-11 were used for this study. Both strains are Gram-positive bacteria, yet *B. simplex* 10w-16b is the only strain that has the endospores' production capability. They were isolated from Panasqueira mine (environment contaminated with metals, mostly W) (Chung, A.P., *et al.* 2019). These strains appear to be promising once they were capable of accumulating tungsten in a previous bioleaching assay (previous results).

1.1. DNA extraction

DNA from the two selected strains was extracted by E.Z.N.A® Bacterial DNA Kit following the indicated in the manufactures' protocol.

2. Genomic analysis

2.1. Phylogenetic tree construction

Based on the nucleotide sequence of the gene coding the 16S rRNA of the selected strains, a phylogenetic tree for each strain was constructed to identify phylogenetically the nearest strains' genomes. NCBI BLAST (Blastn) bioinformatics toll was used to obtain all the similar sequences (with similarity percentage from 93% to 100%). For each strain, all selected sequences were then aligned by ClustalW (MEGA7, Kumar, S., *et al.* 2016). Maximum likelihood with 500 bootstraps replication and partial deletion was the algorithm used to reconstruct the phylogenetic trees.

2.2. Bioinformatic screening of tungsten/molybdenum genes coding for transporter systems and other genes responsible for metal mobilization

Nearest strains were determined by proximity on the phylogenetic tree, by the calculated distances on MEGA7 and by their complete genome's availability on JGI IMG/M genomes database. The identified phylogenetically nearest strains' complete genomes were obtained in the genomes database and the evaluation of the presence of metals mobilization genes was performed by two different strategies: i) Searching by name and function of the respective gene in the nearest strain's genomes on JGI/IMG genomes database; and ii) Blast against genomes with the FASTA protein sequence of all the interesting genes available on BacMet database (Pal, C., *et al.* 2014). The FASTA sequences of search resulting genes were downloaded and aligned on BioEdit (Hall, T., *et al.* 2011) by Multiple Align by ClustalW. The sequences of the genes of interest already described on strains of the same species of the selected strains, and available on the NCBI database, were used as a control to determine the homology between the sequences and infer about their similarity.

3. Detection of specific genes by polymerase chain reaction (PCR) amplification

3.1. Screening of *modA* genes from ModABC transporter system

The amplification of *modA* gene on both selected strains was performed by Polymerase Chain Reaction (PCR), using specific and degenerated primers, as described in **Table 3**.

Table 3. Forward and reverse specific and degenerated primers sequence designed for amplification of *modA* gene from *B. simplex* 10w-16b and *C. cellasea* 10w-11.

Bacterial strain	Gene target	Primers	Designation	Sequence
<i>B. simplex</i> 10w-16b	<i>modA</i>	Specific	Bac.modA'f	5' - CGATAATGATGCTTGTGA TAG - 3'
			Bac.modA'r	5' - CCGTTTGGAGATAGTCAT AGAATAG - 3'
		Degenerated	Bac.deg.modA'f	5' - TDGADGAAGATCTKATTG
			Bac.deg.modA'r	5' - TYTGSAGATARTCATARA
<i>C. cellasea</i> 10w-11		Specific	Cell.modA'f	5' - CTGCTCGTGCGGCCGA
			Cell.modA'r	5' - CCAGGACGAGGATCACG ACCGC - 3'
		Degenerated	Cell.deg.modA'f	5' - TKYWKGC GGCGGAGC CTG - 3'
			Cell.deg.modA'r	5' - RTKGMKCTGSTGSKSAGC GM - 3'

The specific primers for both strains were designed based on the sequence of *modA* genes identified by Blast against the genome on the JGI IMG/M genomes database. The degenerated primers were designed based on several sequences of *modA* genes available on the NCBI database belonging to the same species with 97.34% of similarity in the case of *B. simplex* 10w-16b and with 99.60% of similarity in the case of *C. cellasea* 10w-11, always against the *modA* gene sequence present in their genome.

The PCR gene amplification was performed in a 200µL Eppendorf with a final volume of 30µL, using a thermocycler MyCycler™ (Bio-Rad). **Table 4** shows the composition of each PCR.

Table 4. Composition of PCR for amplification of *modA* gene from both bacterial strains.

Composition	Volumes (µL)
Sterile water (performed)	19.75
MasterMix*	6.25
Primer forward, 0.5 microgram per milliliter (µg/µL)	1.0
Primer reverse 0.5µg/µL	1.0
DNA	2.0

* MasterMix - NZYtaq II 2× Green Master Mix (0.2 U/µL) (dNTPs, 2.5 mM of MgCl₂)

Conditions and the expected length of the amplification product of *modA* gene of both selected strains are summarized in **Table 5** and **Table 6**, using specific and degenerated primers, respectively.

Table 5. Detailed PCR programs with specific primers.

Bacterial strain	Gene target	Amplification conditions		Expected amplified fragment length
<i>Bacillus simplex</i> 10w-16b	<i>modA</i>	1 cycle	Initial denaturation 95 °C for 5min	725 bp
		30 cycle	Denaturation 95 °C for 45sec	
			Annealing 52 °C for 1min	
			Extension 72 °C for 45sec	
		1 cycle	Final extension 72 °C for 10min	
			Final hold 4°C for an indefinite time	
<i>Cellulomonas cellasea</i> 10w-11	<i>modA</i>	1 cycle	Initial denaturation 95 °C for 5min	684 bp
		30 cycle	Denaturation 95 °C for 45sec	
			Annealing 62 °C for 1min	
			Extension 72 °C for 45sec	
		1 cycle	Final extension 72 °C for 10min	
			Final hold 4°C for an indefinite time	

Table 6. Detailed PCR programs with degenerated primers.

Bacterial strain	Gene target	Amplification conditions		Expected amplified fragment length
<i>Cellulomonas cellasea</i> 10w-11	<i>modA</i>	1 cycle	Initial denaturation 95 °C for 5min	684 bp
		30 cycle	Denaturation 95 °C for 45sec	
			Annealing 60 °C for 1min	
			Extension 72 °C for 45sec	
		1 cycle	Final extension 72 °C for 10min	
			Final hold 4°C for an indefinite time	

A negative control was prepared simultaneously with the reaction mixture to detect contamination. PCR amplification products were analyzed through electrophoresis on agarose gel at 1% (w/v) stained with ethidium bromide (10 mg/mL, Bio-Rad) in TAE 1x buffer for 40min

(75volts (V)). The PCR products were purified from the gel (E.Z.N.A.® Gel Extraction Kit) and then sent for sequencing (Stabvida, Portugal).

3.2. Evaluate *modA* genes neighborhood on *B. simplex* 10w-16b

To determine if the two selected strains include in their genome the genes coding for the complete ModABC transporter system, PCR reactions were performed using specific primers (**Table 7**) designed for the two *modA*-following proteins, mentioned in the database JGI IMG/M genomes database, as *hypothetical protein 1* and *hypothetical protein 2*. PCR amplification products were analyzed through electrophoresis on agarose gel at 1% (w/v) and sent for sequencing as mentioned before. To analyze if the *modA* gene, in *B. simplex* 10w-16b, was followed by the hypothetical protein genes (*modB* and then *modC* gene) PCR amplification with Bac.1/2*modA*'f (designed based in the middle of the *modA* gene sequence amplified in *B. simplex* 10w-16b) and Bac.hip2'r designed primers was performed.

Table 7. Forward and reverse specific primers sequence designed for amplification of *hypothetical protein 1* and *hypothetical protein 2* from *B. simplex* 10w-16b.

Gene target	Primers	Designation	Sequence
1/2 <i>modA</i> gene	forward	Bac.1/2ModA'f	5' - ATCGGATCGCTGGAAGACCTC - 3'
<i>hypotetical protein 1</i>	forward	Bac.hip1'f	5' - TCTCATTGTAGTCATGTTA - 3'
	reverse	Bac.hip1'r	5' - GTGCTCGGCTCATAGTAAGT - 3'
<i>hipotetical protein 2</i>	forward	Bac.hip2'f	5' - ATTAATCGTATGTATATCGA - 3'
	reverse	Bac.hip2'r	5' - GTGCTCGGCTCATAGTAAGT - 3'

The PCR gene amplifications were performed as described above, according to the PCR composition shown in **Table 4**.

Table 8. Detailed PCR programs with specific primers for *hypothetical protein 1* and *hypothetical protein 2* separately on *B. simplex* 10w-16b.

Gene target	Amplification conditions		Expected amplified fragment length
<i>hipotetical protein 1</i>	1 cycle	Initial denaturation 95 °C for 5min	334 bp
	30 cycle	Denaturation 95 °C for 30sec	
		Annealing 49 °C for 1min	
		Extension 72 °C for 30sec	
	1 cycle	Final extension 72 °C for 10min	
		Final hold 4°C for an indefinite time	
<i>hipotetical protein 2</i>	1 cycle	Initial denaturation 95 °C for 5min	437 bp
	30 cycle	Denaturation 95 °C for 30sec	
		Annealing 52 °C for 1min	
		Extension 72 °C for 30sec	
	1 cycle	Final extension 72 °C for 10min	
		Final hold 4°C for an indefinite time	

Table 9. Detailed PCR programs with specific primers for half of *modA* gene and both hypotheticals on *B. simplex* 10w-16b.

Gene target	Amplification conditions		Expected amplified fragment length
half of <i>modA</i> gene and both hypotheticals	1 cycle	Initial denaturation 95 °C for 5min	1230 bp
	30 cycle	Denaturation 95 °C for 1min	
		Annealing 60 °C for 1min	
		Extension 72 °C for 1min30seg	
	1 cycle	Final extension 72 °C for 10min	
		Final hold 4°C for an indefinite time	

The expected length of the amplified fragment as well as the conditions are mentioned in **Table 8** for the amplification of both hypothetical genes separately and in **Table 9** for the amplification of an half of *modA* gene and both hypotheticals.

The analyses through electrophoresis, product fragment purification and sequencing was performed as mentioned above.

3.3. Sequencing and gene sequencing analysis

The amino acid sequence was performed by Sanger Sequencing Technique, a service obtained by Stabvida (Coimbra, C., *et al.* 2017).

All sequences were compared with sequences available in NCBI database, using BLAST network services (Blastx) (Altschul, S.F., *et al.* 1990).

The sequences obtained were identified based on the criteria closest sequence and percentage (%) of similarity.

4. Minimum Inhibitory Concentration (MIC) assay

The MIC test can be defined as the lower concentration of any antimicrobial agent that prevents visible microbial growth after incubation (Curtin, J., *et al.* 2003). Reasoner's 2A agar (R2A) medium was prepared with different concentrations of sodium tungstate dehydrate ($\text{Na}_2\text{WO}_4 \cdot 2\text{H}_2\text{O}$) (Sigma-Aldrich) at 3 millimolar (mM), 5mM, 10mM, 20mM, 50mM and 100mM. Sodium molybdate dehydrate ($\text{Na}_2\text{MoO}_4 \cdot 2\text{H}_2\text{O}$) (BDH) was also prepared at the same concentrations. Analytical-grade salts of tungsten (W) and molybdenum (Mo) were prepared as 0.5M stock solutions and sterilized by filtration.

Bacterial suspensions were prepared in 5mL of Phosphate Buffered Saline (PBS) (8 g/l NaCl, 0.2 g/l KCl, 1.44 g/l Na_2HPO_4 , 0.24 g/l KH_2PO_4 , pH 7.4) with an equivalent optical density (OD) of 0.5 in McFarland scale. Then, these suspensions were added to the R2A agar plates. As a control, it was used plates with R2A medium in the absence of the metal solutions. After applying the suspensions in all the plates, they were incubated at 25°C for five days. The growth was evaluated on the third and fifth days of incubation.

5. Tungsten and molybdenum bacterial accumulation assays

The W and Mo accumulation assays were performed for the two selected strains, *B. simplex* 10w-16b and *C. cellasea* 10w-11.

5.1. Growth curve in the presence of metals

The growth of both strains was followed over time in a batch system, in the absence and the presence of W and Mo. Both metals were supplemented at two different concentrations (1 and 5mM for both). To accomplish this, *B. simplex* 10w-16b cells grown in the R2A Broth medium (R2A-B) were used as inoculum. *C. cellasea* 10w-11 was grown in LB medium (10 g/L triptone, 5 g/L yeast extract, 5 g/L NaCl). The cells were diluted 1:10 in 100mL of R2A-B and LB medium, respectively, and then incubated in a shaking incubator at 25°C with an agitation of 140 rotation per minute (rpm) for 24h and 48h, respectively. Cultures in the stationary phase of growth were transferred to 300mL Erlenmeyer flasks containing spiked medium (R2A-B and LB medium in the case of *B. simplex* 10w-16b and *C. cellasea* 10w-11, respectively) with: i) medium without metal (control); ii) 1mM of W; iii) 5mM of W; iv) 1mM of Mo; and v) 5mM of Mo. Initial OD of the cultures was 0.06 at 600nm. The cultures were incubated in a shaking incubator with the same conditions as above. The OD_{600nm} of each culture sample was periodically collected and determined in a spectrophotometer (ThermoScientific).

5.2. Uptake of tungsten and molybdenum during growth

After determining the growth curve, and based on the results for each strain, the ability to accumulate W and Mo from the medium was determined for *B. simplex* 10w-16b and *C. cellasea* 10w-11, at three different points of bacterial growth: i) beginning of the exponential phase; ii) middle of the exponential phase; and iii) end of the exponential phase.

Pre-inoculums and culture inoculations were prepared as described before (point 6.1 of the Methodologies sector) in Erlenmeyer flasks supplemented with: i) 1mM of W; ii) 5mM of W; iii) 1mM of Mo; and iv) 5mM of Mo. All cultures started with initial turbidity of 0.06 OD_{600nm}, and the incubation conditions were the same as described before. At each point of the growth curve (beginning, middle and end), 20mL of cell culture was harvested to a sterile 50mL Falcon tube. Tubes were centrifuged for 20 min, at 4°C and maximum rotation. The supernatant was discarded and the pellets were resuspended in half of the initial volume of PBS solution (10mL). This washing protocol was repeated 3 times at the same conditions. Washed pellets were resuspended in 2mL of PBS solution.

5.3. Tungsten and Molybdenum uptake competition assay

To evaluate the specificity of selected strains to bioaccumulate W and/or Mo, both strains were grown in the presence of the two mixed metal oxyanion solutions. Cells were recovered in the growth phase that had previously presented the highest W/Mo accumulation (determined in point 6.2 of the Methodologies sector). Inoculums and cultures were prepared as described before (point 6.1 of the Methodologies sector). Cultures initial turbidity was adjusted to 0.06 OD_{600nm}. *B. simplex* 10w-16b was grown in three different conditions: i) 5mM of Mo and 0mM of W; ii) 5mM of Mo and 5mM of W; and iii) 5mM of Mo and 10mM of W, being W the competitor metal in this experience. *C. cellasea* 10w-11 it was grown at the same conditions as *B. simplex* with W as the competitor metal, and it was grown in different conditions, when Mo was the competitor metal: i) 5mM of W and 0mM of Mo; ii) 5mM of W and 5mM of Mo; and iii) 5mM of W and 10mM of Mo. At the exponential phase of each culture growth, 20mL of cell culture was harvested to a sterile 50mL Falcon tube. Tubes were centrifuged for 20 min, at 4°C and maximum rotation. The washing process was performed as mentioned above and the pellets were resuspended in 2mL of PBS solution.

5.4. Bacterial cells metal contents

5.4.1. Cell digestion by acid lysis

To each pellet, resulting from the accumulations mentioned above, was added 1mL of nitric acid (HNO₃) 10%, 1:1 (500 µL H₂O + 500 µL HNO₃) followed by incubation in a bath at 50°C for 60 minutes (min). The digested samples were incubated on ice for 30 min and centrifuged for 20min at maximum rotation. In samples resulting from W accumulations, the digested pellet was resuspended in 1mL of PBS solution, once W precipitates in contact with acid. In samples from Mo accumulations, 1mL of the digested supernatant was directly transferred to a new Eppendorf.

5.4.2. Protein quantification through Bradford Method

Protein was quantified from the digested cells (pellets) resuspended with PBS solution. The protein quantification was made through Bradford Method (Kruger, N.J., *et al.* 2009), which uses the Bovine Serum Albumin (BSA) as standard protein control.

20 μ L of the previous resuspended digested cells were transferred to a new Eppendorf with 5 μ L of sodium hydroxide (NaOH) 1M, to neutralize. Quantification was performed in a cuvette by adding 1mL of Bradford reagent, 90 μ L of milli-Q water and 10 μ L of the respective sample. Bradford Reagent only in 100 μ L of milli-Q water was used as a control. Cuvettes were incubated in the dark, at room temperature, for 15min. The absorbance was read at 595nm and the amount of protein was calculated based on the standard curve line ($y = 0.0412x + 0.061$).

5.4.3. Tungsten and molybdenum measurements

The quantification of intracellular metal accumulation in each sample was determined by Inductively Coupled Plasma Mass Spectrometry (ICP-MS). All samples were normalized by the total protein mass.

5.5. Protein expression analysis

To evaluate the protein expression of both strains, *B. simplex* 10w-16b and *C. cellulosa* 10w-11, was performed a 0.1% sodium dodecyl sulfate-12% polyacrylamide gel (SDS-PAGE) in the absence and presence of W/Mo. Both strains were grown as previously described, in the presence of 1mM and 5mM of W and Mo, separately. As a control, strains were grown in the absence of the metal. 50mL of each overnight culture cell was harvested to a 50mL Falcon tube and centrifuged for 20min at maximum rotation. The supernatant was discarded, and the pellet was washed with 25mL of PBS solution. The washing process was repeated 2 times and the washed cells were then resuspended in PBS solution (minimum volume required: 2 mL).

5.5.1. Cell lysis

The cells were lysed by incubation (overnight) in a 37°C bath with 100 μ L of lysozyme 10mg/mL. Incubation was followed by five cycles of 15min of thermal shock (temperatures alternating from -20°C to 40°C). The samples were then centrifuged for 15min at maximum rotation, in order to obtain the soluble protein in the supernatant. Protein quantification was made as mentioned before, through the Bradford Method.

5.5.2. SDS-PAGE and sample preparation

The SDS-PAGE was performed based on the Bio-Rad protocol. All samples added to SDS-PAGE were normalized to the same concentration of protein (13 μ g of total protein), with the

addition of 7 μ l of Loading Buffer (with β -mercaptoethanol) as well as ultrapure water to a final volume of 25 μ l. The prepared samples were incubated at 100°C for 5min, then loaded and evaluated by electrophoresis on a SDS-PAGE and ran at 140volts (V) for 40min.

Coomassie blue staining (2.5g of Coomassie Brilliant Blue R, 454 mL of methanol, 96 mL Acetic Glacial Acid, 450 mL distilled water), previously pre-heated at 50°C, was performed with incubation of approximately 30min, followed by a destaining step (250 mL of methanol, 75 mL Acetic Glacial Acid, 675 mL distilled water) of 45min. The step was repeated with fresh destaining solution every 45min until the gel was clear.

6. Bacterial bioleaching assays

6.1. Monitoring pH variation during bioleaching assay with two different culture media

The pH variation during leaching assays with the two selected strains, grown in two different culture medium (R2A Broth and MBM (Mody-Bam-SM)), was followed. Inoculums for both strains, *B. simplex* 10w-16b and *C. cellasea* 10w-11, were prepared as mentioned above. Cells in stationary phase were transferred to 300mL Erlenmeyer flasks, containing: i) 100mL of R2A Broth medium; and ii) 100mL of MBM medium. All flasks were prepared in an adequate volume to reach the initial turbidity of 0.1 OD_{600nm}. As a control, flasks with 100mL of each culture media were used. The cultures were incubated in a shaking incubator at 25°C at 140rpm for 15 days. 5mL samples were harvested every five days to measure pH.

6.2. Tungsten bioleaching determination

B. simplex 10w-16b and *C. cellasea* 10w-11 were tested for their ability to leach wolframite and Panasqueira mine tailings.

Cells of both strains were obtained as mentioned before. Cultures in stationary phase were transferred to different 300mL Erlenmeyer flasks, containing: i) 1g of wolframite; and ii) 1g of Panasqueira mine tailings, followed by three sterilization cycles by autoclaved (120°C for 20min). Both flasks with 100mL of MBM medium were inoculated with a volume to reach the initial turbidity of 0.1 OD_{600nm}. As controls were used Erlenmeyers with the same quantity as before of: i) wolframite; and ii) Panasqueira Mine tailings, with the same volume of the medium. The cultures were incubated in a shaking incubator at 25°C at 140rpm for 21 days. Samples were harvested at: i) beginning of the incubation (t₀); ii) 7 days after the incubation (t₇); iii) 14 days after the incubation (t₁₄); and iv) 21 days after the incubation (t₂₁), i.e. at the end of the incubation.

6.2.1. The impact of a physical barrier during tungsten bioleaching assays

The impact of a physical barrier between bacterial cells and the tailings on bioleaching and on bioaccumulation performance of the strains was determined. This was achieved by the addition of a membrane filter to the bioleaching assays already stated in point 7.2 of the Methodology sector. The membrane filter, made by a paper filter with a pore size of $2\mu\text{m}$, was introduced in each Erlenmeyer flask already containing 1g of wolframite and 1g of Panasqueira mine tailings, separately, as show in **Figure 7**. The sterilization process was done as mentioned before.



Figure 7. Example of an Erlenmeyer with 1g of Panasqueira mine tailings and a paper filter acting as a physical membrane between the bacterial cells and the mine tailings.

Cultures in the stationary phase were transferred to Erlenmeyer flasks with 100mL of MBM medium and in an adequate volume to reach the initial turbidity of 0.1 $\text{OD}_{600\text{nm}}$. As a control, it was used: i) 1g of wolframite with the paper filter; and ii) 1g of Panasqueira mine tailings with the paper filter. All flasks had the same volume of MBM medium and were incubated under the same conditions as before for 21 days. Samples were harvested at the same points of incubation as above.

6.3. Bioleaching samples treatment

From all samples from all bioleaching assays, at the sampling times mentioned, were removed: i) 2mL to evaluate the presence of metals in the leachate; and ii) 2mL to evaluate the

metal accumulation. The leachate samples were centrifuged at maximum rotation for 15min and the supernatant was transferred to a new Eppendorf tube. In samples from bioaccumulation experiments, after centrifugation, the pellet was resuspended with 1mL of PBS solution. The cells were digested by acid lysis and quantified for total protein by the Bradford Method, as mentioned. The quantification of metals in both leachate and bioaccumulation samples was performed by ICP-MS.

7. Confirmation of bioleaching capacity of a selected strain in Lab-scale lysimeters

Previous to this experiment strains were evaluated for bioleaching capability to select the most promising bioleaching strain. The selected strain was used in lab-scale lysimeters experiments (composed of two columns) to mimic leaching tailings in Panasqueira mine environment.

The system was assembled and filled with Panasqueira mine tailings mixed in a 1:1 ration with quartz sand (0.1 – 0.4mm), with a total mass of 2Kg and left overnight to settle. In the day 1 of the assay, the columns were filled with MBM medium until saturation and left overnight. An inoculum of the most promising bioleaching strain was prepared to be inoculated in column 1 in a bioaugmentation strategy with 0.1 of OD_{600nm}. Column 2, the negative control, was biostimulated with MBM medium. Immediately after the inoculation, the first flushing sample was obtained by direct flow from the bottom of the column. Samples were always removed from both columns. Water pore samples (i.e. retained liquid in the sediment) were removed from the top of the column through a suction cup inserted in the tailings sediments. Sample was obtained applying negative pressure with a vacuum pump (Ψ). Soil samples were also harvested from two different depth points of the column, using a Pasteur pipette, for soil samples from the top of the column and an inverted disposable pipette for soil samples from the middle of the column.

The Lab-scale lysimeters assay was performed during 20 days. Both columns were saturated with fresh MBM medium on days 1, 8, 11, 15 and 18, and left overnight. Flush samples were collected on days 2, 9, 12, 16 and 19 of the assay. The suction cup samples and sediment samples were collected on days 3, 5, 8, 10 and 17 of the assay. The pH was measured in the water pore and flushing samples, and metals quantification was performed by ICP-MS.

Results

1. Genomic Analysis

1.1. Phylogenetic tree construction

The phylogenetic trees constructed for each strain in order to determine the nearest selected strain's genomes are represented in **Figure 8** and **Figure 9**.

The phylogenetically nearest strains were determined according to the calculated distance matrix on MEGA7. The nearest strains to *B. simplex* 10w-16b, whose genomes were available on JGI IMG/M genomes database, were *B. simplex* NBRC 15720 DSM 1321, with a pairwise distance of 99.8%, and *B. muralis* strain LMG 20238 with 98.1%. The nearest strains to *C. cellasea* 10w-11, whose genomes were also available on JGI IMG/M genomes database, were *C. cellasea* DSM 20118 with a pairwise distance of 99.9%, *C. humilata* strain ATCC 25174 with 97.2% and *C. xylanilytica* strain XIL11 with 95.4%.



Figure 8. *B. simplex* strain B1. S5. 4.2 10w-16b phylogenetic tree.

Molecular Phylogenetic analysis by Maximum Likelihood method. The evolutionary history was inferred by using the Maximum Likelihood method based on the Jukes-Cantor model. The bootstrap consensus tree inferred from 500 replicates is taken to represent the evolutionary history of the taxa analyzed. Branches corresponding to partitions reproduced in less than 50% bootstrap replicates are collapsed. The percentage of replicate trees in which the associated taxa clustered together in the bootstrap test (500 replicates) are shown next to the branches. Initial tree(s) for the heuristic search were obtained automatically by applying Neighbor-Join and BioNJ algorithms to a matrix of pairwise distances estimated using the Maximum Composite Likelihood (MCL) approach, and then selecting the topology with superior log likelihood value. The analysis involved 91 nucleotide sequences. All positions with less than 95% site coverage were eliminated. That is, fewer than 5% alignment gaps, missing data, and ambiguous bases were allowed at any position. There were a total of 837 positions in the final dataset. Evolutionary analyses were conducted in MEGA7.

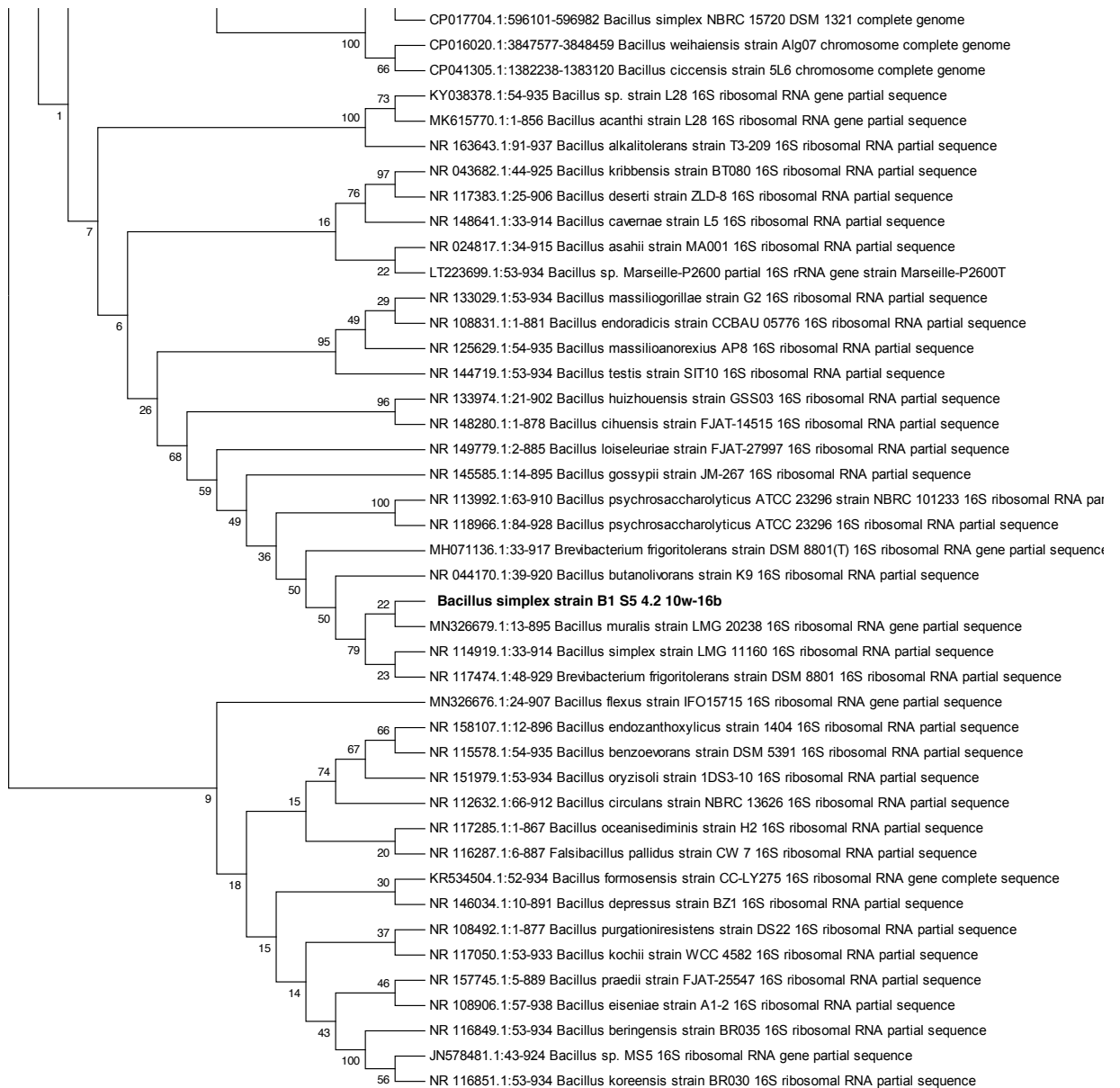


Figure 8. *B. simplex* strain B1. S5. 4.2 10w-16b phylogenetic tree (continuation of the previous figure).

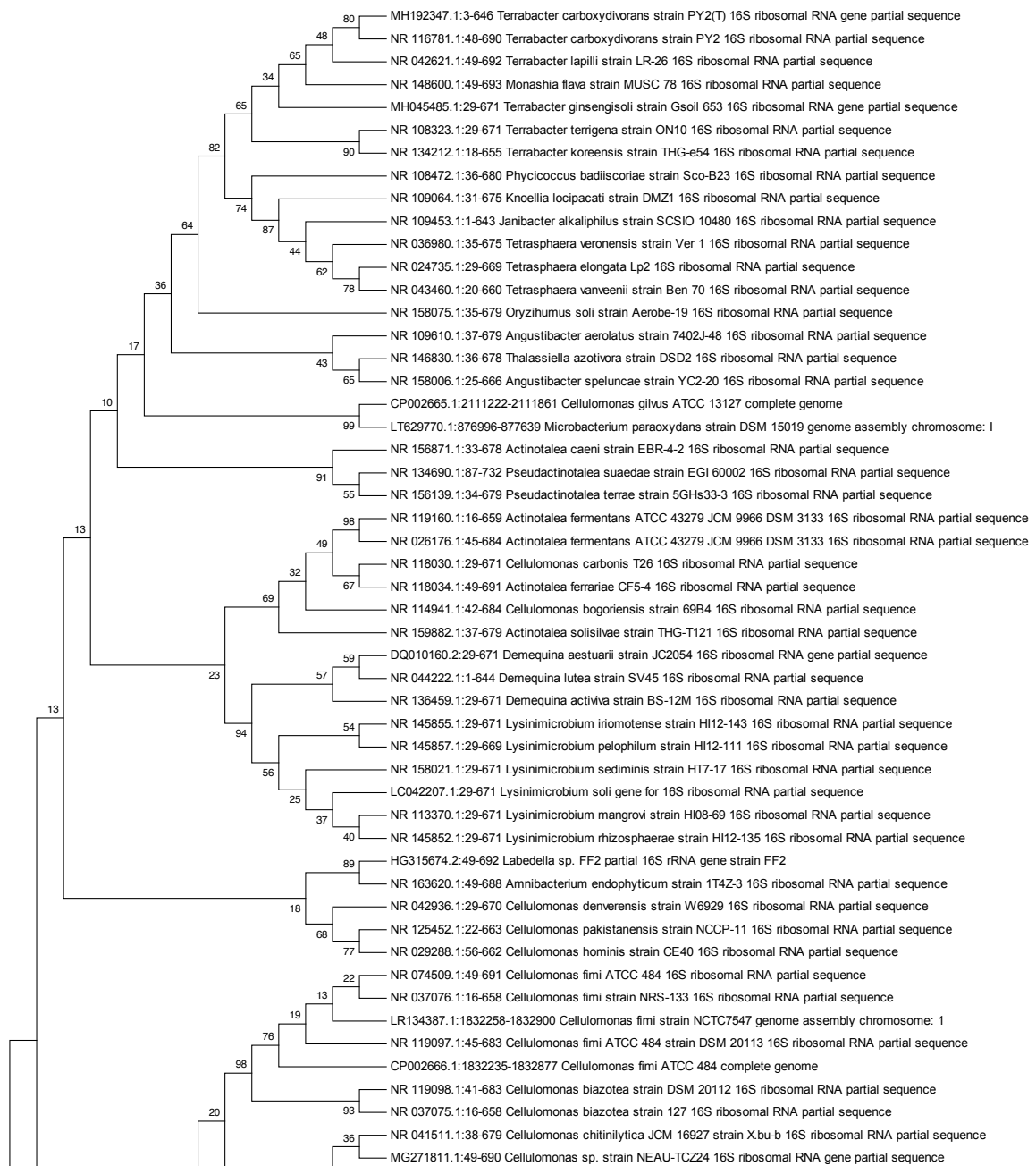


Figure 9. *C. cellasea* strain B2. S3. 2.2 10w-11 phylogenetic tree.

Molecular Phylogenetic analysis by Maximum Likelihood method The evolutionary history was inferred by using the Maximum Likelihood method based on the Jukes-Cantor model. The bootstrap consensus tree inferred from 500 replicates is taken to represent the evolutionary history of the taxa analyzed. Branches corresponding to partitions reproduced in less than 50% bootstrap replicates are collapsed. The percentage of replicate trees in which the associated taxa clustered together in the bootstrap test (500 replicates) are shown next to the branches. Initial tree(s) for the heuristic search were obtained automatically by applying Neighbor-Join and BioNJ algorithms to a matrix of pairwise distances estimated using the Maximum Composite Likelihood (MCL) approach, and then selecting the topology with superior log likelihood value.

The analysis involved 98 nucleotide sequences. All positions with less than 95% site coverage were eliminated. That is, fewer than 5% alignment gaps, missing data, and ambiguous bases were allowed at any position. There were a total of 604 positions in the final dataset. Evolutionary analyses were conducted in MEGA7.

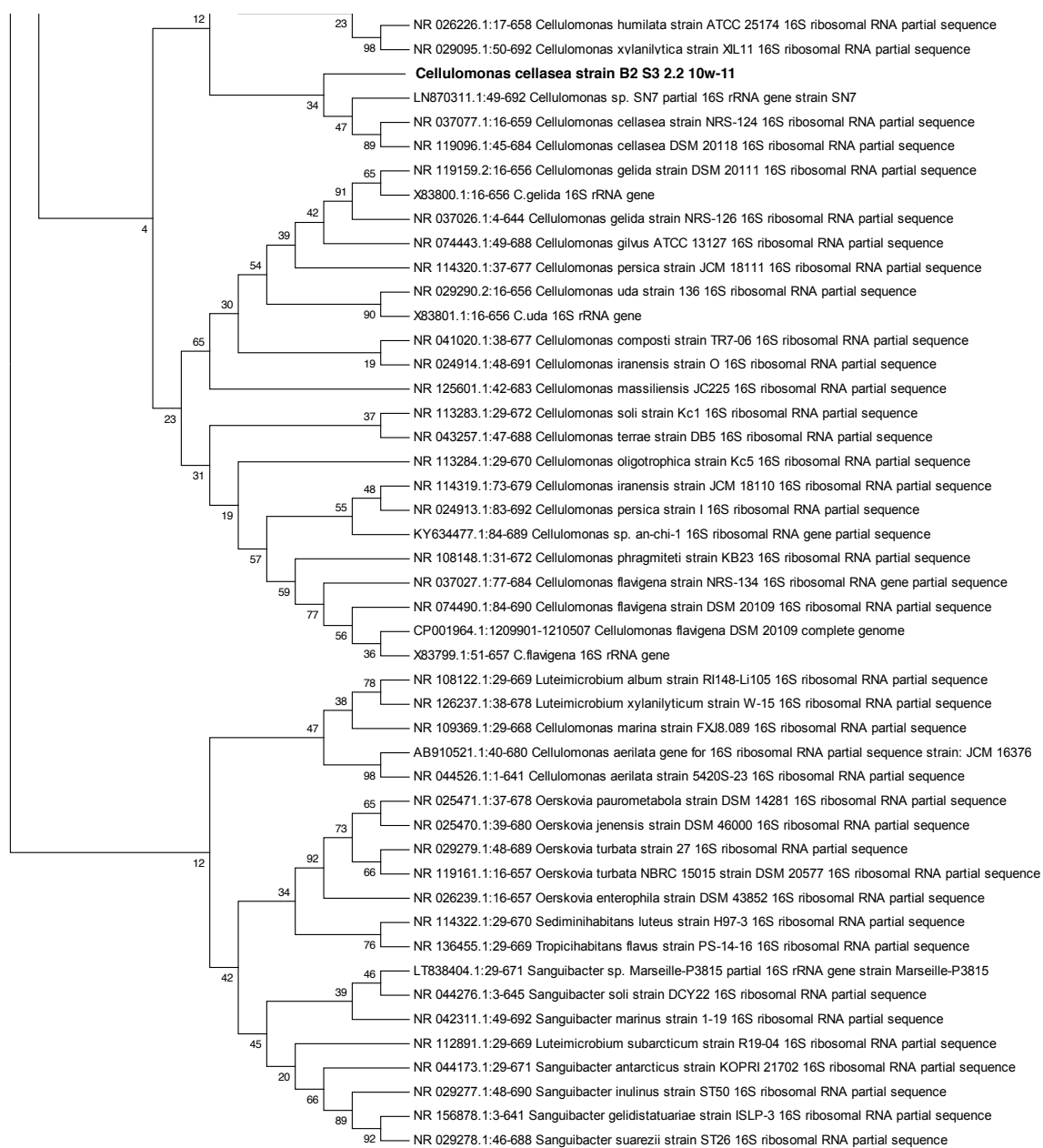


Figure 9. *C. cellasea* strain B2. S3. 2.2 10w-11 phylogenetic tree (continuation of the previous figure).

1.2. Bioinformatic screening of tungsten/molybdenum genes coding transporter systems and searching for other genes of metals mobilization

On JGI IMG/M genomes database, where were available the nearest strains' genomes mentioned above, it was made a search by the function of W resistant genes and transporters by name (keyword), as “permease protein”, and by Blast against genome with those genes' FASTA protein sequences available on BacMet database. These results are listed in **Tables 10** and **11**.

Table 10. Search by name and function of previously identified W resistant genes and transporters on *B. simplex* and *C. cellasea* nearest strains genomes.

Keyword	Organism	Search results	Protein ID
permease protein	<i>Bacillus simplex</i> NBRC 15720)	manganese/zinc/iron transport system permease protein	2732651372
		molybdate transport system permease protein	2732649564
		nickel transport system permease protein	2732652181
		phosphate transport system permease protein	2732650308
		zinc transport system permease protein	2732650295
	<i>Cellulomonas cellasea</i> DSM 20118	manganese transport system permease protein	2633285582
		molybdate transport system permease protein	2633284602
		peptide/nickel transport system permease protein	2633282005
zinc transport system permease protein		633284285	

Table 11. Search by Blast against genome of previously identified W resistant genes and transporters on *B. simplex* and *C. cellasea* nearest strains genomes.

Gene sequence for BLAST (from BacMet database)	Gene ID	Gene product name	Genome name
<i>tupA</i> (<i>Eubacterium acidaminophilum</i>)	2682673431	molybdate transport system substrate-binding protein	<i>Bacillus simplex</i> P558
	2732652417	molybdate transport system substrate-binding protein	<i>Bacillus simplex</i> NBRC 15720
<i>modA</i> (<i>Escherichia coli</i> (strain K12))	2732652417	molybdate transport system substrate-binding protein	<i>Bacillus simplex</i> NBRC 15720
	2823418819	molybdate transport system substrate-binding protein	<i>Bacillus simplex</i> DSM 1321
<i>modA</i> (<i>Escherichia coli</i> (strain K12))	2633284601	molybdate transport system substrate-binding protein	<i>Cellulomonas cellasea</i> DSM 20118

Based on the previous tables, it was possible to determine on the nearest genomes strains of *B. simplex* 10w-16b and *C. cellasea* 10w-11 the presence of a molybdate transporter system by genome bioprospecting. A first approach on the nearest both strains' genomes, by searching by function, allowed to identify the presence of a molybdate transporter system (**Table 10**). Then, Blast against genome with *tupA* protein sequence (available on BacMet) detected a molybdate substrate-binding protein on *B. simplex* 10w-16b nearest strains' genomes. Blast against genome with *modA* protein sequence available on BacMet allowed to confirm the existence of a ModA in both strains' nearest genomes, suggesting the existence of the molybdate transport system (ModABC) (**Table 11**). The detection of *modA* gene on the nearest genome strains and its neighborhood, according to JGI IMG/M genomes database, are in **Figure 10**.

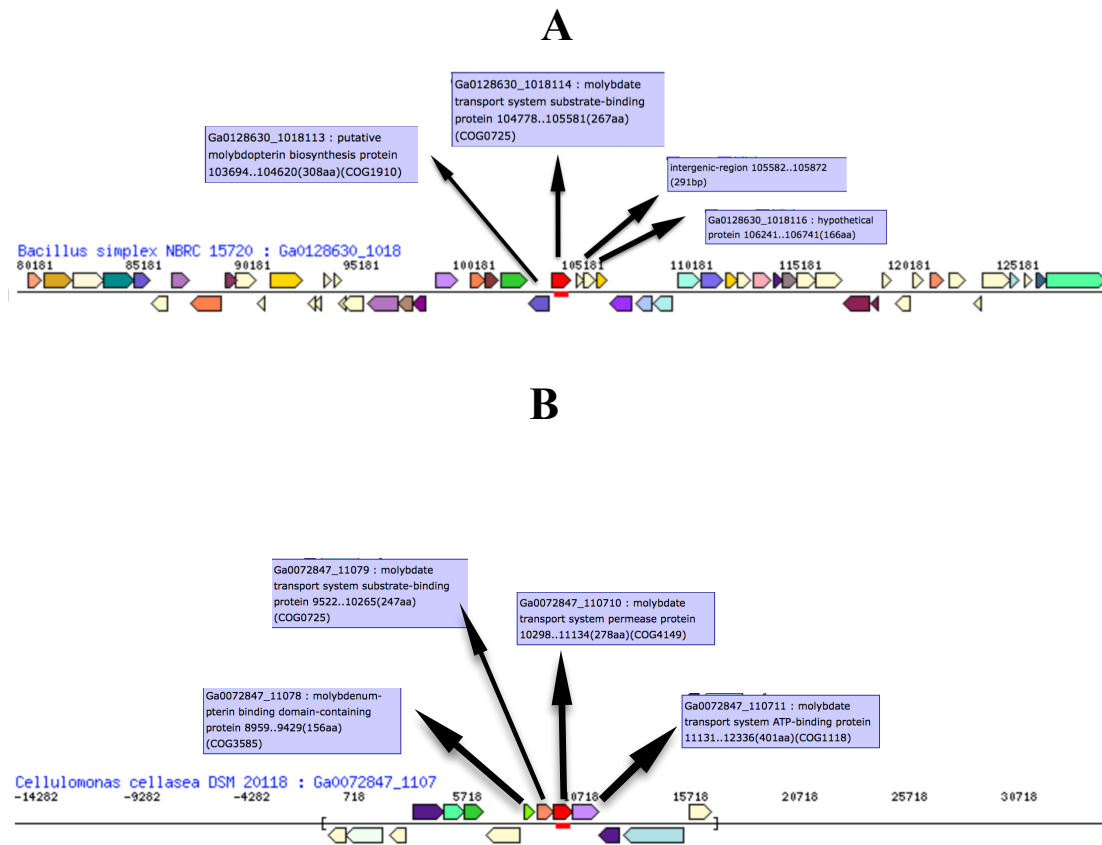


Figure 10. Result for searching by function and by Blast against the nearest *B. simplex* (A) and *C. cellasea* (B) strain's genomes available on the database. Gene's neighborhood available on JGI IMG/M genomes.

2. Detection of specific genes by polymerase chain reaction (PCR) amplification

2.1. Screening of *modA* genes from the ModABC transporter system

Both strains were screened for the presence of *modA* gene, since the bioinformatics analysis suggested the existence of a molybdate transporter in both isolated strains' nearest genomes. Isolated strains were subjected to DNA extraction and PCR amplification. The results, shown in Figure 11, are relatively to *modA* gene amplification on *B. simplex* 10w-16b (**Figure 11.A**) and *C. cellasea* 10w-11 (**Figure 11.B**) with specific primers for both strains, designed based on the sequence of *modA* genes identified by Blast against the genome on the JGI IMG/M genomes database.

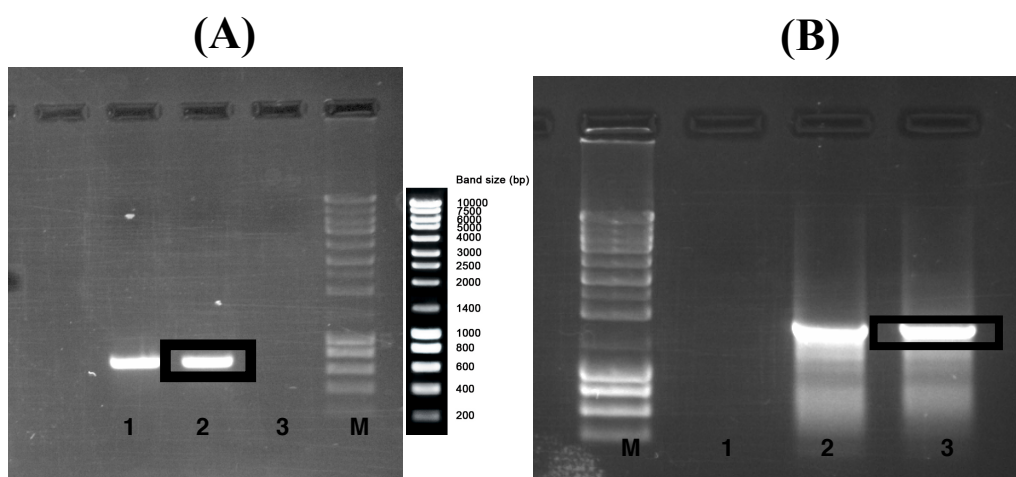


Figure 11. (A) PCR of *B. simplex* s 10w-16b with specific primers on a 1% agarose electrophoresis gel in TAE 1x, stained with ethidium bromide: **well 1**- strain 10w-16b; **well 2**- strain 10w-16b duplicated; **well 3**- negative control; **M**- 4 μ l of NZYTech DNA Ladder III. (B) PCR of *C. cellasea* 10w-11 with specific primers on a 1% agarose electrophoresis gel in TAE 1x, stained with ethidium bromide: **M**- 4 μ l of NZYTech DNA Ladder III; **well 1**- negative control ; **well 2**- strain 10w-11; **well 3** -strain 10w-11 duplicated.

The bands obtained from the PCR with specific primers of *B. simplex* 10w-16b in **Figure 11.A** correspond to the fragment length expected, 725 base pairs (bp) (bands are between 600bp and 800bp, but closer to the 800bp). Therefore, the PCR product of *B. simplex* 10w-16b (band in the black box) was purified and sent to sequencing and the fragment showed a sequence similarity of 97% with a molybdate-binding protein. Therefore, *B. simplex* 10w-16b has *modA* gene in its genome.

From the PCR amplification with the specific primers in the case of *C. cellasea* 10w-11, it was expected a band with a fragment length of 684bp. However, as shown in **Figure 11.B**, the obtained band in the black box did not have a fragment length as expected according to the bioinformatic analysis, resulting in an inconclusive amplification. The existence of a molybdate substrate-binding coding gene in *C. cellasea* 10w-11 could not be confirmed. Therefore, a second PCR amplification for this strain was performed with degenerated primers (**Figure 12**) designed based on several sequences of *modA* genes available on the NCBI database belonging to the same species. For this PCR amplification, was also expected a band with a fragment length of 684bp and, once again the results were not conclusive about the existence of the *modA* gene in this strain, since the resultant PCR product did not have the expected fragment length.

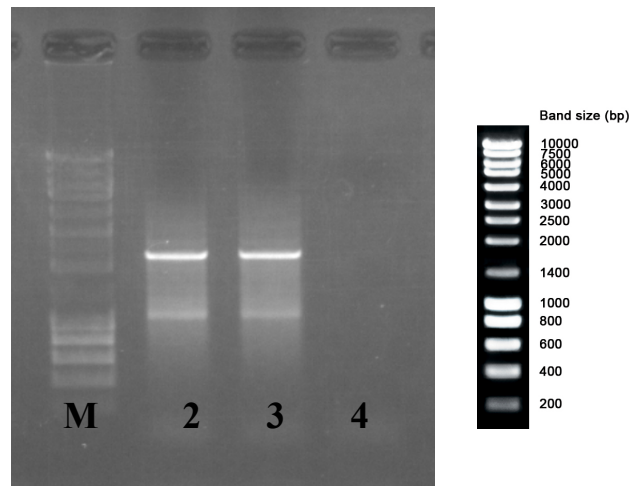


Figure 12. PCR of *C. cellasea* 10w-11 with degenerated primers on a 1% agarose electrophoresis gel in TAE 1x, stained with ethidium bromide: **M**- 4µl of NZYTech DNA Ladder III; **well 2**- strain 10w-11; **well 3**-strain 10w-11 duplicated; **well 4** - negative control.

In the genome of *B. simplex* 10w-16b nearest strains, as shown in **Figure 10**, according to the JGI IMG/M genomes database, the gene *modA* (molybdate transport system substrate-binding protein) was followed by two other genes, not identified yet and so indicated as hypothetical genes in the database, we inferred that could be *modB* and *modC*.

In order to determine if the *B. simplex* 10w-16b included in the genome the other genes coding for the complete ModABC transporter system, primers designated as hypothetical 1 and 2 were designed based on the sequence of the two *modA* following genes indicated as hypotheticals in the database. **Figure 13** show the results from the amplification of the two *modA* following genes, according to JGI IMG/M genomes database, *hypothetical protein 1* and *hypothetical protein 2*, separately.

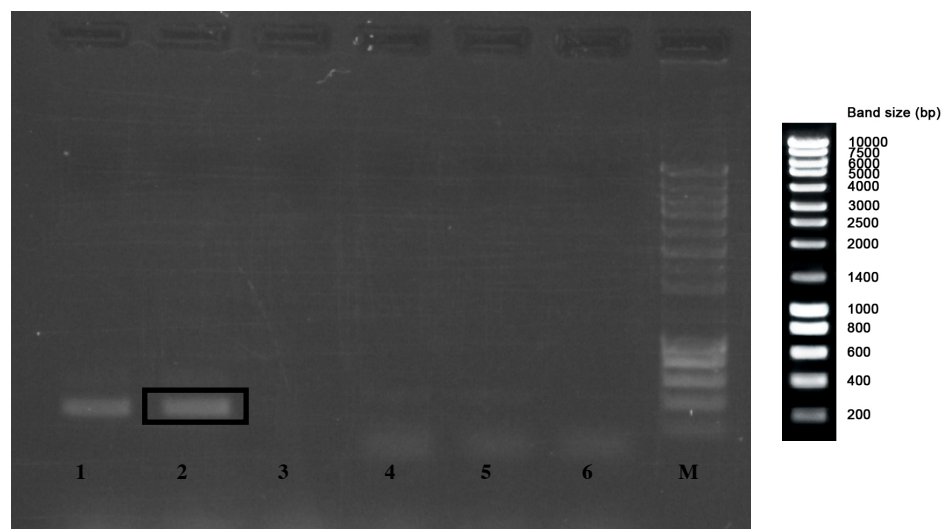


Figure 13. PCR of *B. simplex* 10w-16b with specific primers for *hypothetical protein 1* and *2* separately on a 1% agarose electrophoresis gel in TAE 1x, stained with ethidium bromide: **well 1**- strain 10w-16b primers *hip1FeR*; **well 2**- strain 10w-16b duplicated primers *hip1FeR*; **well 3**- negative control; **well 4**- strain 10w-16b primers *hip2FeR*; **well 5**- strain 10w-16b duplicated primers *hip2FeR*; **well 6**- negative control; **M**- 4µl of NZYTech DNA Ladder III.

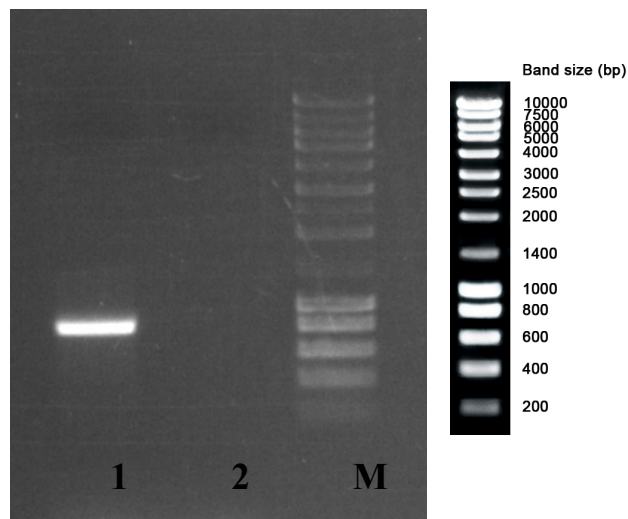


Figure 14. PCR of *B. simplex* 10w-16b with specific primers for *hypothetical protein 1* and *2* together on a 1% agarose electrophoresis gel in TAE 1x, stained with ethidium bromide: **well 1-** strain 10w-16b; **well 2-** negative control; **M-** 4 μ l of NZYTech DNA Ladder III.

The amplification of *hypothetical protein 1*, with the expected length of 334bp according to the bioinformatics analysis, resulted in a fragment with that length as it was expected (between bands of 200bp and 400bp, but closer to 400bp). The PCR product of *B. simplex* 10w-16b (band in the black box) was purified and sent for sequencing. The BLAST result showed a sequence similarity of 97.00% with a *Bacillus simplex* hypothetical protein.

The PCR amplification of *hypothetical protein 2* did not result in bands as show in **Figure 13**. The amplification using a second set of primers to amplify a fragment with both hypotheticals genes together (*hypothetical 1* and *hypothetical 2*) was performed (**Figure 14**). The amplicon with the fragment length expected (805bp), (black box) was purified and sent to sequencing. The BLAST result showed a sequence similarity of 98.68% with a *Bacillus simplex* hypothetical protein.

In order to analyze if the *modA* gene, in *B. simplex* 10w-16b, was followed by the hypothetical protein genes by the order of *modB* and then *modC* gene, PCR amplification with Bac.1/2modA'f and Bac.hip2'r primers was performed (**Figure 15**).

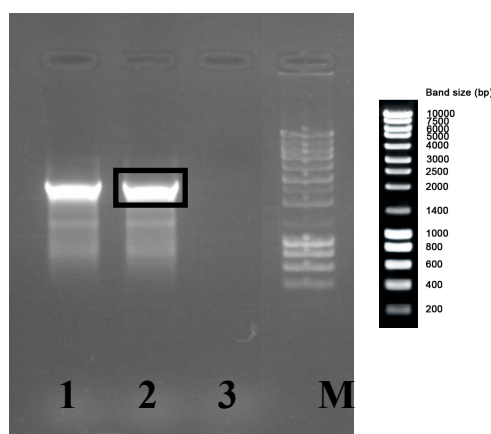


Figure 15. PCR of *B. simplex* 10w-16b with specific primers for half of *modA* gene and *hypothetical protein 2* on a 1% agarose electrophoresis gel in TAE 1x, stained with ethidium bromide: **well 1**- strain 10w-16b; **well 2**- strain 10w-16b duplicated; and **well 3**- negative control. **M**- 4 μ l of NZYTech DNA Ladder III.

It was expected a fragment length of 1230bp. The amplification resulted in a fragment between bands of 2000bp and 2500bp, but closer to 2500bp. The band (black box) was purified and sent for sequencing. BLASTp showed a protein sequence similarity of 100% with molybdate substrate-binding protein. A blast of the obtained PCR product with the known *modA* gene of *B. simplex* NBRC 15720 was performed. This Blast allowed us to find that the first part of the gene (fragment length of 665bp) was highly conserved, 100% homologous with the *B. simplex* NBRC 15720 *modA* gene with 801bp. The rest of the amplified fragment showed to be a sequence similarity of approximately 60% with a hypothetical protein.

3. Characterization of the strains as resistant to tungsten and molybdenum

Both selected strains, isolated from Panasqueira Mine, were characterized by its potential to resist to tungsten (W) (**Table 12**) and to molybdenum (Mo) (**Table 13**). The Minimum Inhibitory Concentration (MIC) assay was used to evaluate strains' resistance.

Table 12. MIC results of the two selected strains, isolated from Panasqueira Mine, at different concentration of W after 3 and 5 days of incubation. +: grow, - does not grow, +/- doesn't grow very well.

		3 days					
	Control (-)	3mM W	5mM W	10mM W	20mM W	50mM W	100mM W
<i>B. simplex</i>	+	+	+	+	+	+	+
<i>C. cellasea</i>	+	+	+	+	+	+	+/-
		5 days					
	Control (-)	3mM W	5mM W	10mM W	20mM W	50mM W	100mM W
<i>B. simplex</i>	+	+	+	+	+	+	+
<i>C. cellasea</i>	+	+	+	+	+	+	+/-

Table 13. MIC results of both selected strains, isolated from Panasqueira Mine, at different concentration of Mo after 3 and 5 days of incubation. +: grow, - doesn't grow, +/- doesn't grow very well.

		3 days					
	Control (-)	3mM Mo	5mM Mo	10mM Mo	20mM Mo	50mM Mo	100mM Mo
<i>B. simplex</i>	+	+	+	+	+	+	+
<i>C. cellasea</i>	+	+	+	+	+/-	-	-
		5 days					
	Control (-)	3mM Mo	5mM Mo	10mM Mo	20mM Mo	50mM Mo	100mM Mo
<i>B. simplex</i>	+	+	+	+	+	+	+
<i>C. cellasea</i>	+	+	+	+	+/-	-	-

The results showed that *B. simplex* 10w-16b after 5 days of incubation was capable of grow at all tested concentrations of both tested metals. Therefore, this strain is resistant to both metals until a concentration of 100mM. However, *C. cellasea* 10w-11 was resistant to W up to a concentration of 50mM, and to Mo up to a concentration of 20mM, being more resistant to W than to Mo. The results show that *B. simplex* 10w-16b is more resistant to both metals than *C. cellasea* 10w-11, which is more resistant to W.

4. Characterization of both strains as accumulators

Strains were characterized considering their ability to accumulate W and Mo according to the Methodologies sector described in paragraph 6.1. **Figure 16** presents the growth curves of each strain, at two different concentrations of W and Mo and without the presence of the metals (designated as the negative control). Both strains were grown at concentrations of 1mM and 5mM for both metals, separately.

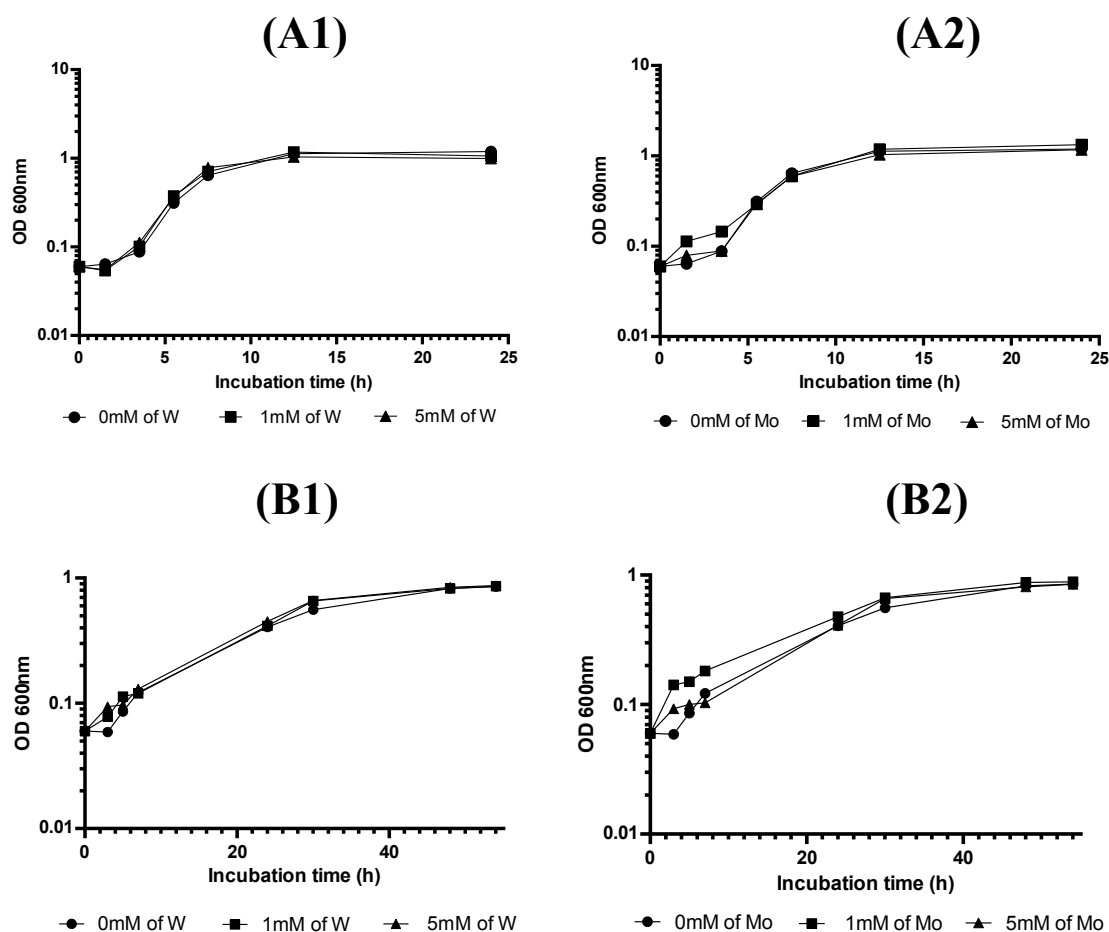


Figure 16. Growth curves of *B. simplex* 10w-16b (A) and *C. cellasea* 10w-11 (B) in the absence and presence of W (A1 and B1) and Mo (A2 and B2) both at concentrations of 1mM and 5mM.

Table 14 shows the specific growth rate (μ) of both strains at the different concentrations of W and Mo.

Table 14. Values of specific growth rate from growth curves of both strains tested, at different concentration of tungsten and molybdenum.

Bacterial strain	Metal	Metal concentration (mM)	Linear regression line	R2	Specific grow rate (μ -1)
<i>B. simplex</i> 10w-16b	W	0	$y = 0.345x - 1.0092$	0,998	0.34
		1	$y = 0.355x - 1.008$	0,999	0.36
		5	$y = 0.321x - 0.870$	0,999	0.32
	Mo	0	$y = 0.345x - 1.0092$	0,998	0.34
		1	$y = 0.366x - 1.100$	0,995	0.37
		5	$y = 0.359x - 1.129$	0,997	0.36
<i>C. cellasea</i> 10w-11	W	0	$y = 0.2307x - 0.792$	0,999	0.23
		1	$y = 0.260x - 0.932$	0,999	0.26
		5	$y = 0.236x - 0.7789$	0,999	0.24
	Mo	0	$y = 0.2307x - 0.792$	0,999	0.23
		1	$y = 0.2377x - 0.759$	0,999	0.24
		5	$y = 0.251x - 0.889$	0,999	0.25

When W and Mo were added to the culture media, no significant alteration was seen for both strains. *B. simplex* 10w-16b shown an higher growth rate in the presence of Mo, at 1mM, at the beginning of its growth than in the absence of this metal. The growth in the presence of W remained stable as the negative control. As show on **Table 14**, the μ for *B. simplex* 10w-16b was higher when W and Mo were at lower concentrations (1mM).

In the case of *C. cellasea* 10w-11, when compared with the other strain, it did not grow much in the presence or absence of both metals. However, its growth is increased by the presence of W and in the presence of Mo in the culture medium. For *C. cellasea* 10w-11, the μ was higher when W was present at lower concentration (1mM) and when Mo was present at higher concentration (5mM).

The results of uptake of W and Mo by *B. simplex* 10w-16b (**Figure 17.A**) and *C. cellasea* 10w-11 (**Figure 17.B**) are show in **Figure 17**. The amount of each metal was determined at three different points of the growth curve: beginning, middle and end of the exponential phase of strains' growth curves. The W and Mo quantification was performed by ICP-MS analysis, as mentioned in the Methodologies chapter.

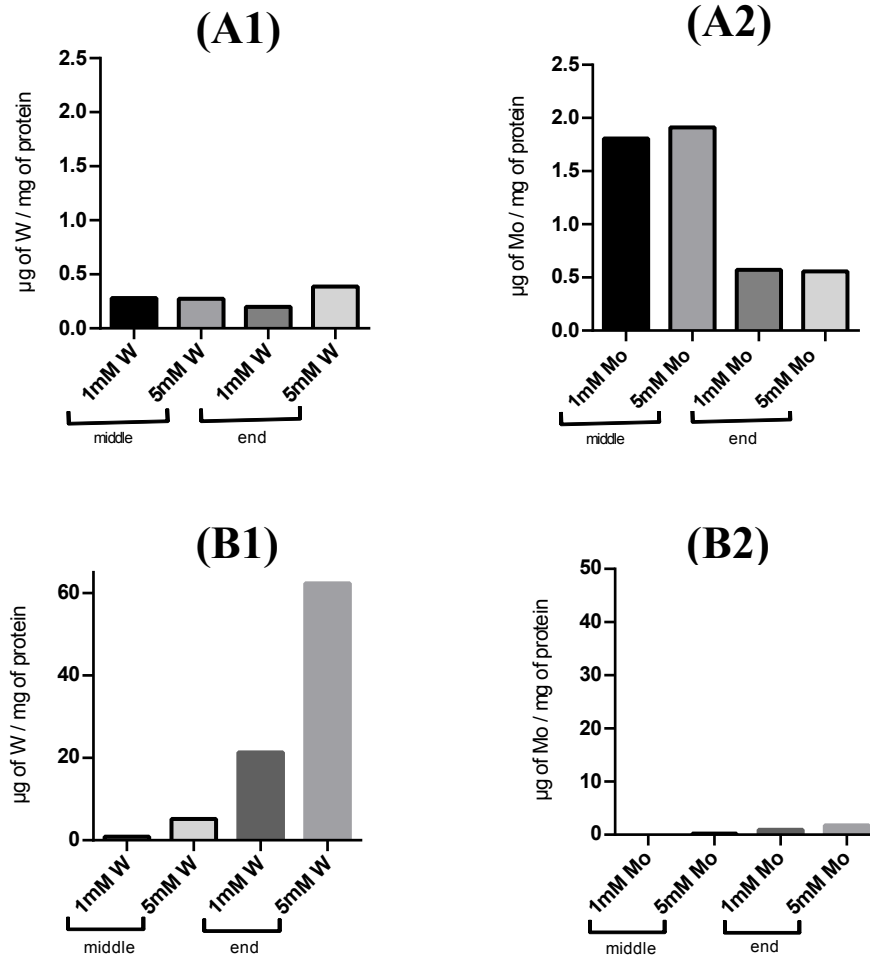


Figure 17. *B. simplex* 10w-16b (A) and *C. cellasea* 10w-11 (B) uptake results for W(A1) and (B1) and Mo (A2) and (B2) at two different concentrations: 1mM and 5mM.

At the beginning of the exponential phase of the growth curve for both strains, it was not possible to quantify protein due to the low quantity of bacterial cells (data not shown). With this, only the uptake results for the middle and the end of the exponential phase for both metals are shown.

ICP-MS results show that *B. simplex* 10w-16b has a maximum uptake of W at the end of the exponential phase of its growth curve (0.39µg of W/mg protein) when the metal is present in the culture medium at the concentration of 5mM. On the other hand, when Mo is present in the culture medium at a concentration of 5mM, *B. simplex* 10w-16b has a maximum uptake in the middle of the exponential phase of its growth, 2 µg of Mo/mg of protein. The accumulation pattern, regarding the uptake values and the timing of the exponential phase of the growth curve, varies from one metal to another.

In the case of *C. cellasea* 10w-11 ICP-MS results show that this strain has a maximum of W and Mo accumulation at the end of the exponential phase of growth, with 60 µg of W/mg protein and 1.8µg of Mo/mg protein, respectively.

The accumulation pattern is equal when comparing the W uptake assay with the Mo uptake assay regarding the timing of the exponential phase of growth. On the other hand, the

uptake values varied from one metal to another. Considering both strains, the amount of metal accumulated by the cells is higher at high environmental concentrations, for both tested metals.

4.1. Tungsten and molybdenum accumulation competition assay

Both strains were grown in the presence of both metals, W and Mo, to understand the specificity of each metal to bioaccumulate. Cells from *B. simplex* 10w-16b growth were harvested at the point of its growth phase that had previously presented the highest W/Mo accumulation, i.e. in the middle of the exponential phase of the growth curve. In the case of *C. cellasea* 10w-11 cells were harvested at the end of the exponential phase of the growth curve. The next figures show the results for accumulation competition assay for *B. simplex* 10w-16b (**Figure 18**) as well as for *C. cellasea* 10w-11 (**Figure 19**).

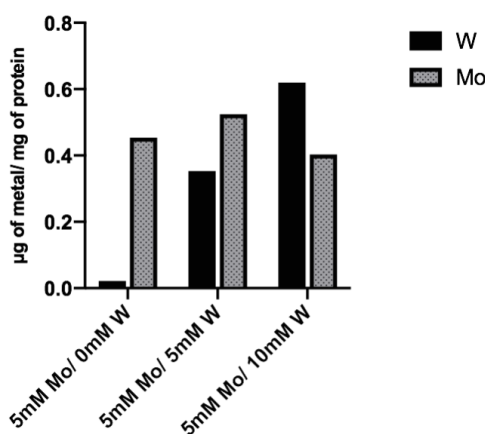


Figure 18. Uptake competition assay for *B. simplex* 10w-16b where W was the competitor metal and the three experimental conditions were: i) 5mM of Mo and 0mM of W; ii) 5mM of Mo and 5mM of W; and iii) 5mM of Mo and 10mM of W. Cells were recovered at the middle of the exponential phase of the growth curve.

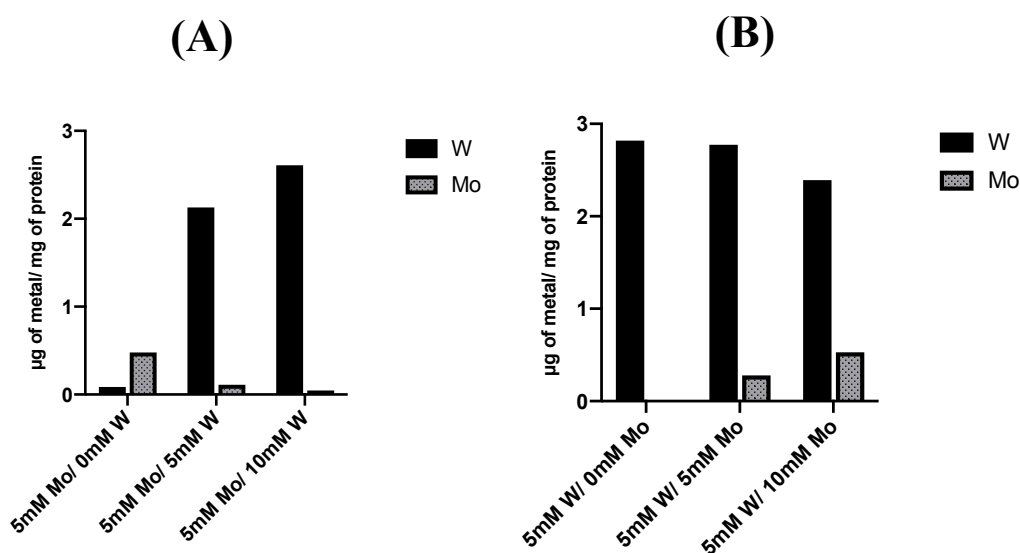


Figure 19. Uptake competition assay for *C. cellasea* 10w-11: (A) W was the competitor metal and the three experimental conditions were: i) 5mM of Mo and 0mM of W; ii) 5mM of Mo and 5mM of W; and iii) 5mM of Mo and 10mM of W. (B) Mo was the competitor metal and the three experimental conditions were: i) 5mM of W and 0mM of Mo; ii) 5mM of W and 5mM of Mo; and iii) 5mM of W and 10mM of Mo. Cells were recovered at the end of the exponential phase of the growth curve.

B. simplex 10w-16b, has the *modA* gene detected by PCR as show previously, and with this, to confirm if this strain had higher affinity for Mo, it was done a competition accumulation assay where W was the competitor metal. *B. simplex* 10w-16b, as shown in **Figure 18**, when in the presence of the same concentration of both metals, accumulated preferentially Mo. Nevertheless, this strain can also accumulate W, especially when the competitor metal is available at higher concentration than Mo, as shown in the third experimental condition (grown in the presence of 5mM of Mo and 10mM of W).

PCR amplification from *C. cellasea* 10w-11 DNA did not enable to conclude if this strain has the *modA* gene. Two different competition accumulation assays were done with W as the competitor metal (**Figure 19.A**) and Mo as the competitor metal (**Figure 19.B**). This strain showed high specificity to bioaccumulate W in both assays. When W and Mo are in the culture medium at equal concentrations - 5mM, *C. cellasea* 10w-11 has a preference to bioaccumulate W instead of Mo. This specificity for W by this strain is corroborated by the uptake values shown in the third experimental condition (5mM of W and 10mM of Mo), in **Figure 19.B**, when the competitor metal is Mo. Even in this case, with Mo present in the culture medium in two times the concentration of W, *C. cellasea* 10w-11 demonstrated the capability of bioaccumulating 0.528 µg of Mo/mg of protein, but shows a high specificity for W, by accumulating 2,4 µg of W/mg of protein.

5. Analysis of protein expression in the absence and presence of tungsten and molybdenum

Both strains, highly resistant to W and Mo, were grown in the presence and absence of both metals to analyze the protein expression profile. The SDS-PAGE gels were obtained for *B. simplex* 10w-16b (**Figure 20.A**) and *C. cellasea* 10w-11 (**Figure 20.B**).

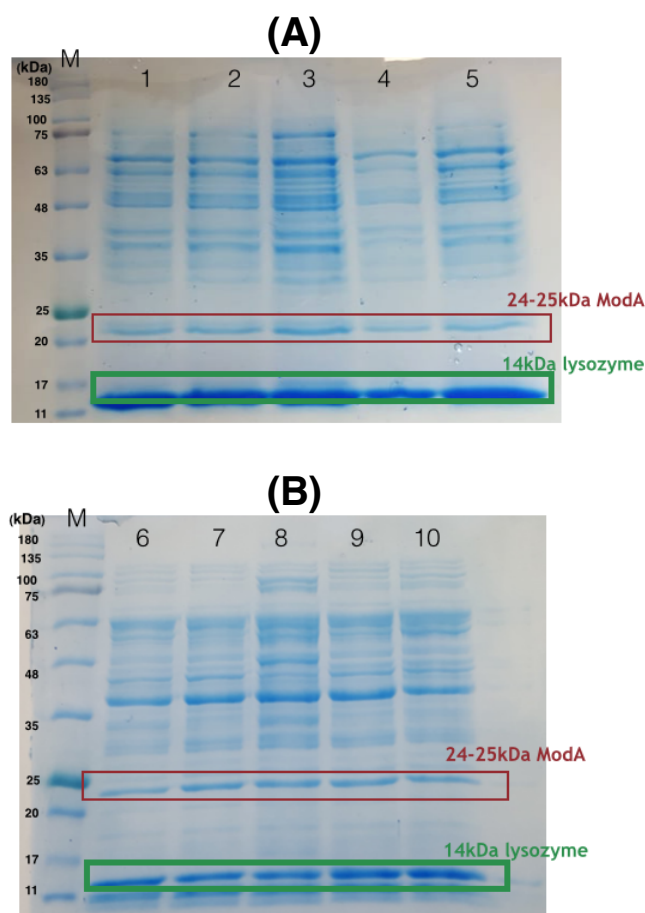


Figure 20. (A) - Results of electrophoresis SDS-PAGE (12%) of the protein profile of *B. simplex* 10w-16b growth with W and Mo at 1mM and 5mM. **well 1**- strain 10w-16b, **well 2**- strain 10w-16b with 1mM W, **well 3** - strain 10w-16b with 5mM W, **well 4** - strain 10w-16b with 1mM Mo and **well 5** - strain 10w-16b with 5mM Mo. **(B)** - Results of electrophoresis SDS-PAGE (12%) of the protein profile of *C. cellasea* 10w-11 growth with W and Mo at 1mM and 5mM. **well 6**- strain 10w-11, **well 7** - strain 10w-11 with 1mM W, **well 8**- strain 10w-11 with 5mM W, **well 9** - strain 10w-11 with 1mM Mo, and **well 10** - strain 10w-11 with 5mM Mo.

From the figures presented above, it is possible to observe bands with 14 kDa corresponding to Lysozyme protein (Wu, H., et al. 2015). This is in concordance to the cell lysis protocol that included a lysozyme solution. The ModA protein, which was consistent with the size predicted from the amino acid sequence (24 kDa) (Sigel, A., et al. 2002), is equally expressed in the absence and presence of both metals, in both concentrations, on both strains. Furthermore, there is no difference in the protein expression profile, both in the presence and in the absence of W or Mo, which suggests that protein expression in both strains is not regulated.

6. Characterization of each strain regarding their capability to bioleach

6.1. Bioleaching's culture media determination assay

To determine which culture media was the most indicated to the bioleaching assays, a pH variation study was performed during strains growth in two culture media, R2A and MBM, was done. This assay was made with both strains as well as with the Panasqueira mine tailings. The pH values are summarized in **Table 15**.

Table 15. R2A and MBM culture medium's pH variation during 15 days in a leaching assay with both selected strains and Panasqueira mine tailings.

	pH T ₀		pH T ₅		pH T ₁₀		pH T ₁₅	
	R2A	MBM	R2A	MBM	R2A	MBM	R2A	MBM
Control (-)	6,800	5,900	5,781	6,009	5,500	5,970	5,871	5,830
<i>B. simplex</i> <i>10w-16b</i>	6,700	6,000	8,787	4,565	8,630	4,684	8,957	4,522
<i>C. cellasea</i> <i>10w-11</i>	6,655	5,948	7,863	4,376	8,005	4,536	8,511	4,300

The pH in R2A medium during the bioleaching assay, started at pH around 6, increased to values between 8 and 9. High pH values will precipitate all metals. On the other hand, the pH from MBM medium remains the same values without variations during the experiment. We can see that this medium is keeping the environment acid, is indicated for the bioleaching assays. So, the MBM medium was chosen to perform all the following bioleaching assays.

6.2. Bioleaching assay with wolframite or with Panasqueira mine tailings

B. simplex 10w-16b and *C. cellasea* 10w-11 were tested for their ability to metal mobilization from solid material (wolframite and Panasqueira mine tailings), focusing on the metal concentration mobilized into the bacterial cells (accumulated) and metal leached to the medium.

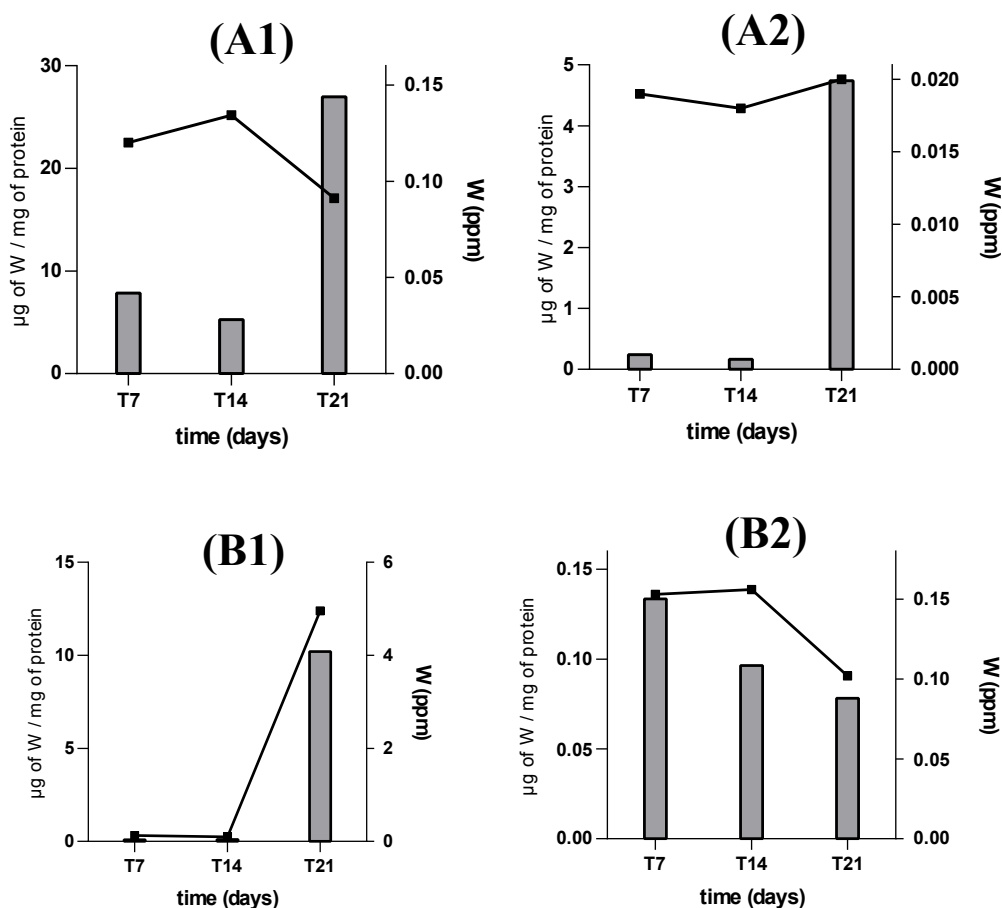


Figure 21. ICP-MS results of W uptake during bioleaching assay for *B. simplex* 10w-16b (A) and *C. cellasea* 10w-11 (B), with wolframite (A1 and B1) and Panasqueira mine tailings (A2 and B2). The W mobilized to the medium in ppm is also shown in line on the right y axis on the graphs.

During the bioleaching assays, the samples were collected periodically and analyzed by ICP-MS. **Figure 21** presents the results for the W concentration into the bacterial cells during bioleaching assay and the W concentration mobilized to the liquid culture medium for both strains with wolframite and with Panasqueira mine tailings. **Table 16** presents these bioleaching values for W with its respective percentage of W in the culture medium.

On the bioleaching assay with *C. cellasea* 10w-11 and wolframite (**Figure 21.B1**) it was observed a high accumulation of W of 10.2 μ g of W/mg of protein at the end of the assay's 21 days (t21). This amount was 10-fold the amount leached the others experimental days (t7 and t14). However, in the other bioleaching assay with the same strain but with the Panasqueira mine tailings (**Figure 21.B2**), there is no significant accumulation of this heavy metal inside the cells during the assay, once the higher uptake value inside the cells in this experimental condition is 0.133 μ g of W/mg of protein. This strain accumulates more W at the beginning of the assay (t7) and decreases over time until the end of the experiment. Although accumulating low concentration of W in Panasqueira mine tailings, *C. cellasea* 10w-11 has the ability to highly accumulate W from wolframite concentrated, mostly at the end of the experiment. When comparing both assays, wolframite and Panasqueira mine tailings, the accumulation pattern for this strain at this bioleaching process is different.

B. simplex 10w-16b (**Figure 21.A1**), the mobilization of W from the wolframite (**Figure 21.A2**) was also possible to observe. During the experiment, high accumulation of W was detected at the end of the assay (21 days (t21)) with uptake values of 26.9 μ g of W/mg of protein. This corresponds to almost a 20-fold W concentration compared with the experimental day t14. The accumulation of 4.74 μ g of W/mg inside the cells during the bioleaching assay with *B. simplex* 10w-16b and Panasqueira mine tailings (**Figure 21.A2**) showed a significant uptake into the cells of W after 21 days of the experiment (t21), with almost 5-fold when compared with the other experimental days (t7 and t14). *B. simplex* 10w-16b had the ability to accumulate W from Panasqueira mine tailings and wolframite concentrated, mostly at the end of the experiment. When comparing wolframite and Panasqueira mine tailings assays, the accumulation pattern for this strain when incubated with solid metal is similar. Nevertheless, the accumulation of W is lower when incubated with Panasqueira mine tailings than with wolframite.

Table 16. W mobilized to the medium and its respective percentage for *B. simplex* strain 10w-16b and *C. cellasea* strain 10w-11 with wolframite concentrated and Panasqueira mine tailings.

Bacterial strain	Leaching assay with:	Time (days)	W ppm	%W leached
<i>B. simplex</i> 10w-16b	Wolframite	t ₇	0.12	0,05
		t ₁₄	0,14	0,06
		t ₂₁	0,091	0,04
	Panasqueira mine tailings	t ₇	0,019	0,14
		t ₁₄	0,018	0,13
		t ₂₁	0,02	0,14
<i>C. cellasea</i> 10w-11	Wolframite	t ₇	0,126	0,05
		t ₁₄	0,1	0,04
		t ₂₁	4,96	0,22
	Panasqueira mine tailings	t ₇	0,158	1,1
		t ₁₄	0,160	1,12
		t ₂₁	0,102	0,73

Leaching percentages were calculated based on W concentrations in Panasqueira mine tailings determined by Chung and colleagues (Chung, A.P., *et al.* 2019). Based on the values of W mobilization to the medium shown in the **Figure 21** and in **Table 16**, *B. simplex* 10w-16b did not mobilized (bioleached) W in the presence of wolframite concentrated, being 0.14 ppm (t₁₄) the maximum concentration of W in the medium. The same occurred during the bioleaching assays with the Panasqueira mine tailings, once the maximum value of W in the medium was 0.02ppm of W after 21 days of the experiment (t₂₁), which corresponds to 0.14% of W bioleached from Panasqueira mine tailings.

C. cellasea 10w-11 showed bioleaching of Panasqueira mine tailings at the two intermediary experimental days (t₇ and t₁₄) of 0.158ppm and 0.160ppm of W mobilized to the medium, respectively. After 21 days bioleaching (t₂₁), this strain was capable to mobilize 4.96 ppm of W to the medium when incubated with wolframite, and 0.102 ppm of W when incubated with Panasqueira mine tailings. *C. cellasea* 10w-11 can bioleach 1.12% of W from Panasqueira mine tailings. So, this strain showed to be better W bioleacher when using Panasqueira mine tailings than wolframite.

B. simplex 10w-16b did not show the ability to bioleached other metals (data not shown) when grown with Panasqueira mine tailings. Only *C. cellasea* 10w-11 showed the ability to bioleach other metals besides W, as Zinc (Zn), Silica (Si) and Copper (Cu) during the bioleaching assay with Panasqueira mine tailings (**Figure 22**).

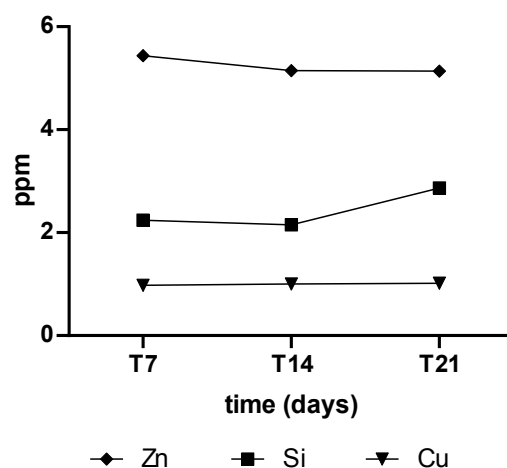


Figure 22. Bioleaching values of other metals besides W like Zn, Si and Cu, during bioleaching assay with *C. cellasea* 10w-11 and Panasqueira mine tailings.

Comparing both strains, *C. cellasea* 10w-11 proved to be the most promising leaching strain, not only because of its capability to bioleach W but also because of its capability to bioleach other metals existing in Panasqueira mine tailings.

6.3. Bioleaching assay using physical barrier (filter paper)

Bioleaching assays using a paper filter as a physical barrier was performed and the samples of cell cultures were also collected periodically. To evaluate the impact of a physical barrier between bacterial cells and the solid material in the metal concentration mobilized into the bacterial cells (accumulated) and metal leached to the medium, samples were analyzed by ICP-MS.

On these bioleaching assays with both strains it was not possible to observe any significant values of bioaccumulation into the cells (data not shown). This indicates that the physical contact between bacterial cells and the ore (wolframite or Panasqueira mine tailings) is necessary for biomobilization of the metal directly from the solid to the cell inside (bioaccumulation).

Table 17 shows the bioleached W values and percentage for both strains, from wolframite and from Panasqueira mine tailings using a filter barrier.

Table 17. W mobilized to the medium and its respective percentage for *B. simplex* strain 10w-16b and *C. cellasea* strain 10w-11 with wolframite concentrated and Panasqueira mine tailings during bioleaching assay with a physical barrier (paper filter).

Bacterial strain	Leaching assay with:	Time (days)	W ppm	%W leached
<i>B. simplex</i> 10w-16b	Wolframite	t ₇	0,0020	0,0009
		t ₂₁	0,0020	0,001
	Panasqueira mine tailings	t ₇	0,0017	0,0007
		t ₂₁	0,00125	0,0005
<i>C. cellasea</i> 10w-11	Wolframite	t ₇	0,0016	0,007
		t ₂₁	0,032	0,014
	Panasqueira mine tailings	t ₇	0,00158	0,0007
		t ₂₁	0,0401	0,0017

Comparing the results shown on **Table 16** with the results of **Table 17** is possible to observe that the W leaching percentage in the medium is much lower when the leaching assay is performed with a paper filter, which indicates that for W mobilization, these strains need physical contact between the bacterial cells and the wolframite or the Panasqueira mine tailings.

7. Preliminary results of bioleaching capacity of a selected strain in Lab-scale lysimeters

Both strains were evaluated for bioleaching capability to select the most promising bioleaching strain. *C. cellasea* 10w-11 was considered to be the most promising leaching strain, based on its capability to mobilize W and Cu and Zn (metals that are present in Panasqueira mine tailings) to the medium. Therefore, this strain was used in lab-scale lysimeters experiments (composed of two columns, **Figure 23**) to mimic leaching tailings in Panasqueira mine environment.

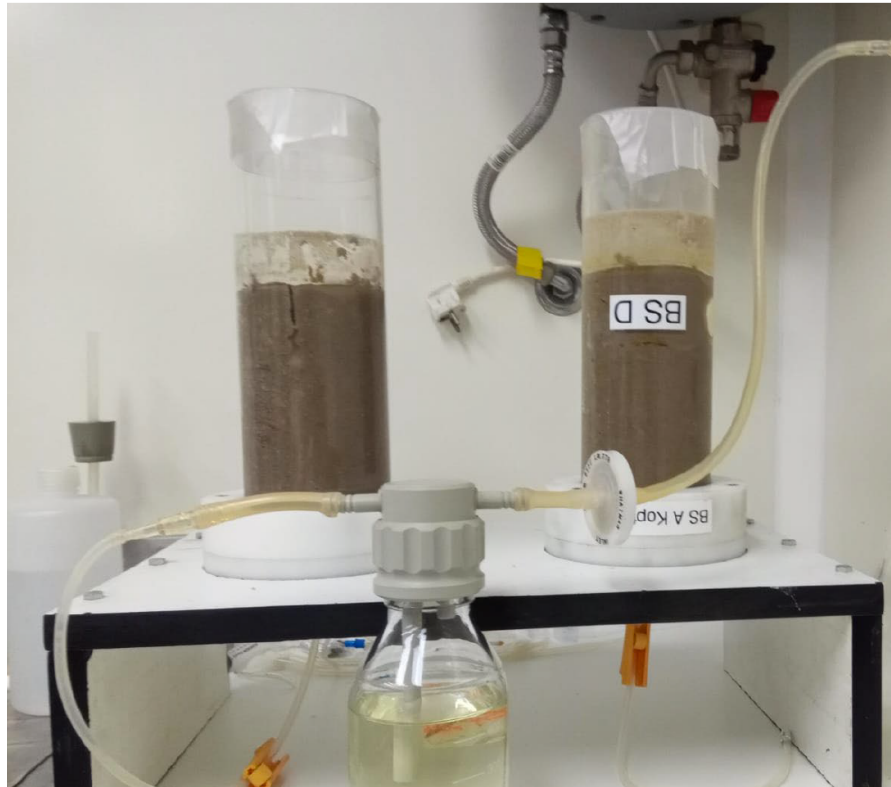


Figure 23. Lab-scale lysimeters composed by two columns, both filled with Panasqueira mine tailings and MBM medium.

Lab-scale lysimeters, as observed in **Figure 23**, were filled with Panasqueira mine tailings and MBM medium. Column 1, following a bioaugmentation strategy, was inoculated with *C. cellasea* 10w-11. Column 2 was only biostimulated with the culture medium, being considered as a negative control, since we aimed to evaluate the strain bioaugmentation effect in metals mobilization to the medium.

Samples were always removed from both columns. Flushing samples were obtained by direct flow from the bottom of the column (percolation water). Water pore samples (i.e. retained liquid in the sediment) were removed from the top of the column through a suction cup inserted in the tailings sediments, and Soil samples were harvested from two different depth points of the column.

The pH was measured in the water pore and flushing samples and these results are presented in **Table 18**.

Table 18. pH variation during the lab-scale lysimeters bioleaching assay measured in flushing samples (F#) and in suction cup samples (SC#).

	pH				
	F# 1	F# 2	F#3	F#4	F# 5
Control (-) (biostimulation)	3,84	4,11	4,10	4,31	4,49
<i>C. cellasea</i> 10w-11 (bioaugmentation)	4,03	4,06	3,97	3,10	4,23
	SC# 1	SC# 2	SC#3	SC#4	SC# 5
Control (-) (biostimulation)	4,12	3,94	3,88	4,19	4,04
<i>C. cellasea</i> 10w-11 (bioaugmentation)	4,25	3,73	3,66	3,77	3,93

As observed in **Table 18**, the pH values in flushing and suction cup samples remain similar during the experiment, keeping the environment acid. This maintenance of the pH values is observed in both columns (bioaugmentation of *C. cellasea* 10w-11 and negative control - biostimulation).

The pH in the beginning of the assay is 6, since the pH of the culture medium MBM is adjusted to that value before autoclaving. The observation of a pH values around 4 in water pore and percolation water during the assay probably results from the activity of the microbial community of tailings, since the tailings are not sterile.

W quantification in the water pore and percolation water was performed by ICP-MS. The preliminary results of metal mobilized to the medium concentrations are summarized on **Table 19**. ICP-MS analysis also detected Se (selenium) mobilized to the medium and these results are shown in **Table 20**.

Table 19. ICP-MS results of W mobilized to the medium in ppb determined in percolation water and water pore samples during lab-scale lysimeters bioleaching assay.

	W (ppb)				
	F# 1	F# 2	F#3	F#4	F# 5
Control (-) (biostimulation)	8,12	6,73	7,37	6,05	9,40
<i>C. cellasea</i> 10w-11 (bioaugmentation)	7,80	6,85	7,63	6,32	10,03
	SC# 1	SC# 2	SC#3	SC#4	SC# 5
Control (-) (biostimulation)	0,007	109,1	7,70	9,59	6,20
<i>C. cellasea</i> 10w-11 (bioaugmentation)	0,0230	5,52	5,20	6,77	11,35

Table 20. ICP-MS results of Se mobilized to the medium in ppm determined in percolation water and water pore samples during lab-scale lysimeters bioleaching assay.

	Se (ppm)				
	F# 1	F# 2	F#3	F#4	F# 5
Control (-) (biostimulation)	1,01	1,244	1,32	1,63	1,90
<i>C. cellasea 10w-11</i> (bioaugmentation)	1,00	1,137	1,195	1,55	1,80
	SC# 1	SC# 2	SC#3	SC#4	SC# 5
Control (-) (biostimulation)	1,98	2,40	2,37	2,56	2,84
<i>C. cellasea 10w-11</i> (bioaugmentation)	1,89	2,12	2,36	2,601	2,77

Based on the preliminary leaching results presented in **Table 19**, the bioaugmentation of *C. cellasea 10w-11* was not effective, once it appears that this strain was not able to mobilize high amounts of W to the culture medium during the bioleaching assays in lab-scale lysimeter. On the other hand, the second water pore sample collected shown that 109.1 ppb of W were mobilized to the medium on the biostimulation column, indicating that the biostimulation of the mine tailings environment could be effective in the promotion of metals mobilization to the medium. However, more leaching and molecular assays are needed for this to be proven.

The results shown in **Table 20** indicate that selenium (Se) was mobilized to the culture medium in both columns (bioaugmentation and biostimulation column). Despite of the autochthonous strain *C. cellasea 10w-11* being capable of mobilize to the medium Cu and Zn in bioleaching assays in batch culture(as shown in **Figure 22**), this capability was not observed during the bioleaching assay in lab-scale lysimeters (data not shown).

Discussion

Tungsten (W) is one of the most important metals with high economic importance and high supply risk, used in many key industries especially in high-tech technology (Coimbra, C., et al. 2017). Worldwide, there are several mines in operation that have large wolframite extraction. Portugal has one of the largest active producers of W concentrates in Europe - the Panasqueira mine, localized in Barroca Grande. The ore processing in Panasqueira mine produces tailings that contain interesting amounts of W and other metals. These tailings are deposited in two basins in the mines' surrounded area, being an environmental concern (Chung, A.P., et al. 2019). Thus, an in-depth understanding of the tailings microbiome and its metabolic capabilities, can provide a direction for the management of tailings disposal sites and maximize their potential as secondary resources through a circular economy perspective (Wang, X., et al. 2019).

Mine tailings are characteristically oligotrophic environments, full of toxic metals, which is a challenge for microbial survival and maintenance. However, in Panasqueira mine tailings, despite the concentration of the high metals, a high diversity of microbial communities playing an important ecological role were identified specially belonging to the family *Anaerolineacea* and genera *Acinetobacter*, *Bacillus*, *Cellulomonas*, *Pseudomonas*, *Streptococcus* and *Rothia* (Chung, A.P., et al. 2019).

The two bacterial strains tested in this study were both isolated from the Panasqueira mine tailings, being considered autochthonous organisms. These two bacterial strains belong to the genera *Bacillus* and *Pseudomonas*, two of the most common genera that colonize Panasqueira mine tailings (Chung, A.P., et al. 2019). In preliminary bioleaching assays, *Bacillus simplex* strain B1. S5. 4.2 10w-16b and *Cellulomonas cellasea* strain B2. S3. 2.2 10w-11 appears to be promising, since they were capable of accumulating W in its most common environmental form – tungstate (WO_4^{2-}). This was an indication that they were capable of mobilizing W from wolframite during the assay and transporting it into the cells, so they could eventually have W transporter systems.

This work aimed to characterize the two autochthonous strains isolated from Panasqueira mine tailings. This was done to get more information to further allow us to understand the role of the mine microbiome in the W mobilization. Moreover, this work wanted to evaluate the use of the mine tailings as secondary sources of metals to be recovered by bioaugmentation using the two autochthonous strains. The firstly, it was perform genome bioprospecting in *B. simplex* 10w-16b and *C. cellasea* 10w-11 to detect genes previously related with metal resistance transporter systems, especially directed to W or Mo. It was possible to amplify the *modA* gene on *B. simplex* 10w-16b's genome. Despite the inconclusive attempt to amplify a *modB* and a *modC* genes by PCR amplification, this result suggests the existence of a ModABC transporter in this strain, belonging to the molybdate (MoO_4^{2-}) uptake transporter family, also transporting WO_4^{2-} (Barajas, E.A., et al. 2011). In the case of *C. cellasea* 10w-11, the PCR amplification of modABC genes was inconclusive. The bioinformatics analysis has indicated the existence of a molybdate

transport system, but the results obtained by PCR and Blast analysis did not corroborate the bioinformatics result.

Metal resistance to W and Mo was one characteristic determined for both strains. The minimal inhibitory concentration (MIC) assays with W and with Mo showed that resistance was different between both strains. *B. simplex* 10w-16b was resistant up to 100mM for W and Mo. Yet, *C. cellasea* 10w-11 was only resistant up to 50mM for W and up to 20mM for Mo. Even if the tested concentrations were very high compared to the Panasqueira mine tailings' concentrations, determined and published in the work of Chung and colleagues (Chung, A.P., et al. 2019), not limiting the growth of *C. cellasea* 10w-11, *B. simplex* 10w-16b is more resistant to both metals than *C. cellasea* 10w-11. These results show both strains resistant to colossal concentrations of both metals. The presence of an uptake system suggests that the bacterial cells needs the metal and uses it in its metabolism (enzymatic cofactor). So these resistance results also show that the *B. simplex* 10w-16b' capability of tolerate high of W and Mo, (mostly Mo) concentrations is consistent with the amplified *modA* gene on *B. simplex* 10w-16b.

W is the heaviest known element with a biological function and it is known that some bacteria can bioaccumulate this metal. To occur the bioaccumulation process, often bacteria require genes coding proteins related to transport systems. These transport systems carry the metals specifically (or not so specifically) into the cells. In this study, it was an objective to deepen the study relative to the uptake of W and Mo into the cells, during the cell growth at different metal concentrations. The results showed that *B. simplex* 10w-16b did not appear to be a good W accumulator since the maximum accumulation value is near to 0.4 μ g W/mg protein. *B. simplex* 10w-16b accumulates low amounts of W comparing with the uptake values of W determined by Coimbra and colleagues (Coimbra, C., et al. 2019) for the strain Eco_tupBCA which could uptake up to 1.41 μ g W/mg protein. On the other hand, strain Eco_tupBCA could accumulate Mo up to 0.84 μ g Mo/ mg protein and the maximum accumulation of this metal for *B. simplex* 10w-16b is 1.91 μ g Mo/mg protein. Comparing with Eco_tupBCA Mo uptake values, this is considered a significant value (1.91 μ g Mo/mg protein), meaning that *B. simplex* 10w-16b is a good Mo accumulator. This Mo accumulation ability was consistent with the amplified *modA* gene on this strain. *C. cellasea* 10w-11, was capable of accumulating Mo, and showed a high capacity to bioaccumulate W at the end of the exponential phase of the growth curve reaching values of 62.29 μ g W/mg protein.

According to Aguilar-Barajas et al., (2011) bacteria can incorporate W and Mo ions, with more or less selectivity, by three known different transport systems, as Mod, Tup and Wtp. These systems are all able to transport Mo and W but each system is more selective for the transport of one of the metals. The preference to bioaccumulate W or Mo for both strains was tested using competition assay. When the two metals where present, Mo was accumulated in higher quantities in the *B. simplex* strain 10w-16b. However, lower quantities of W were also incorporated into the *B. simplex* 10w-16b cells, when grown with both metals in the same concentration. The selective preference of *B. simplex* 10w-16b strain for Mo uptake together with the ability of WO_4^{2-} incorporation in lower amounts may be related to the presence of *modA* gene in this strain. *C.*

cellasea 10w-11 selectively accumulated W in all tested conditions. Quantities of Mo were incorporated into *C. cellasea* 10w-11 cells in vestigial amounts, suggesting the existence of a specific W transporter, as shown by Coimbra *et al.* with uptake competition assays with the strain Eco_tupBCA carrying a TupABC transporter system.

Some bacterial strains have the ability of mobilize metals from solid material, such as ore and tailings, that can be incorporated inside the cells or remain bioavailable in the medium. These abilities can be related to the presence of metals dedicated to accumulating systems or some resistance mechanisms (Anjum, F., *et al.* 2012; Adams, G.O., *et al.* 2015). In this work, we explored protein profiling to relate the presence of specific proteins when cells were grown in metal containing media. As proven in this work, *B. simplex* 10w-16b has a *modA* gene that encodes for ModA protein and the appearance of bands with 24 kDa in the electrophoresis SDS-PAGE (putative ModA protein) corroborates this result. According to the results obtained by SDS-PAGE, this protein was also present in *C. cellasea* 10w-11. The protein weight (24kDa) suggests a protein belonging to an accumulating system, which can be ModA or TupA since proteins from both systems show similar weights (Coimbra, C., *et al.* 2019). Furthermore, there is no difference in the protein expression profile of both strains in the presence or absence of both metals tested, W and Mo, in different concentrations, which seems to indicate that protein expression is not regulated by metal's concentrations in the media.

The efficiency of the bioleaching processes in the removal of metals from contaminated soils and tailings by bacteria can be affected by different parameters especially the medium composition and the pH (Ayangbenro, A.S., *et al.* 2017; Rasoulnia, P., *et al.* 2020). The present work showed that the MBM medium was the most indicated for bioleaching assays, once it allowed maintenance of an indicated pH for bioleaching to occur. High pHs levels in the leachate, that happen when R2A medium is used in bioleaching assays, conduce to metals precipitation limiting the bioleaching processes.

Both culture medium have a similar nutritional composition, differing in the existence of the amino acid Asparagine in medium MBM. The maintenance of the pH with the MBM medium may be due to Asparagine and how this amino acid is metabolized by the two strains. According to KEGG metabolic pathways database (Kanehisa, M., *et al.* 2002), L-Asparagine enters in the metabolic pathway of Alanine, aspartate and glutamate metabolism, leading to the production and consumption of NH_4^+ at the same rate, maintaining the pH in the culture medium constant (Gholamian, S., *et al.* 2013).

The ability of the cells to mobilize the metal directly from the solid ore into the cells during bioleaching assays was a new observation that has to be explored. As mentioned before, during uptake assays with tungstate, *B. simplex* 10w-16b accumulated low amounts of W (0.4 μg W/mg protein). However, during bioleaching assays, this strain was capable of mobilize into the cells 26.9 μg of W/mg of protein from wolframite and 4.74 μg of W/mg from Panasqueira mine tailings, suggesting that mobilization of W into the bacterial cells is higher when occur from solid ore and tailings.

This work showed that *B. simplex* 10w-16b was incapable of bioleaching W and other metals to the medium when in the presence of the ore. Nevertheless, *B. simplex* 10w-16b was a high W and Mo resistant strain with the ability to cell accumulate Mo and W when in contact with wolframite. *C. cellasea* 10w-11 was also able to cell accumulate both metals. This strain showed also to be capable of bioleaching W, as well as other metals as copper and zinc present in the Panasqueira mine tailings, being considered a promising bioleaching strain.

It is known that several factors can affect bioleaching processes, as mentioned before and as shown in this work. The bioleaching assays performed with a membrane filter as a physical separation between bacterial cells and the wolframite or mine tailings showed that cells can mobilize metals directly from solid ore. To do it, these cells need to be in physical contact with the ore. This mobilization performed by *B. simplex* 10w-16b and *C. cellasea* 10w-11 was performed by moving the metal element directly from the ore into the cell, bioaccumulating the metals. These results were a step forward in the understanding of how these two bacterial strains interact with the metals, specifically with W and with Mo.

Bioleaching processes tested with lab-scale lysimeters, are much closer to the real conditions of a particular contaminated site than batch shaking tests, allowing the analysis of various parameters, such as pH, and the collection of solid samples, and percolation water and water pore samples (Grossule, V., *et al.* 2020). Collection of water pore samples is relevant since the metal mobilization occur at the micro level between the bacteria and the ore grain, then the mobilized ion needs to stay in concentration equilibrium to be detected in the flush water. (Grossule, V., *et al.* 2020) Since several factors can affect bioleaching processes, as mentioned before, during the bioleaching assay with lab-scale lysimeters, the pH of collected percolation water and water pore samples was measured. The maintenance of the pH observed corroborate that MBM medium was the most indicated for leaching assays, avoiding pH variations that can affect the bioleaching processes.

Panasqueira ores contains high amounts of W and contains sulfides as shown by Chung and colleagues (Chung, A.P., *et al.* 2019). Selenium is most commonly found as an impurity, replacing a small part of the sulfur in sulfide ores of many metals. Anthropogenic sources of selenium include coal burning, and the mining and smelting of sulfide ores. During bioleaching assays with lab-scale lysimeters, Se was mobilized to the medium from panasqueira mine tailings. Some bacteria contain tungsten-molybdopterin and also non-protein bound selenium, in a tungsten-selenium molybdopterin complex that has not been definitively described (Schröder, T., *et al.* 1999; Graentzdoerffer, A., *et al.* 2003). However, consider this, the mobilization of this metal is expected, since *C. cellasea* 10w-11 has high specificity for tungsten.

Conclusions

For the results presented, some conclusions can be drawn:

- *B. simplex* 10w-16b showed to have the *modA* gene, coding for the molybdenum - binding protein, but the existence of *modB* and *modC* genes was not clarified;
- Both strains characterized in this study are highly resistant to tungsten (W) and molybdenum (Mo), where *B. simplex* 10w-16b is more resistant to both metals than *C. cellasea* 10w-11;
- *B. simplex* 10w-16b presented the capacity to grow better at 1mM of W or Mo in the liquid medium, exhibiting higher growth rates in these conditions. For *C. cellasea* 10w-11, the growth rate is lower when no metal is added to the culture medium, suggesting that W and Mo are used by the cell and do not induce toxicity;
- *B. simplex* 10w-16b showed to accumulate Mo in the cell, especially in the middle of the exponential phase of the growth curve;
- *C. cellasea* 10w-11 showed to accumulate W, especially in the end of the exponential phase of the growth curve;
- Cells of *C. cellasea* 10w-11 and *B. simplex* 10w-16b had a maximum accumulation ability when grown in the presence of 5mM of W or Mo, respectively;
- When grown in the presence of both metals in liquid medium, *B. simplex* 10w-16b showed high specificity for Mo and *C. cellasea* 10w-11 for W;
- Growth in the presence or absence of W and Mo in different concentrations does not change the protein expression profile studied by SDS-PAGE in both strains;
- The components of culture medium and the way how they are metabolized interfere with the pH of the culture medium, which can interfere with the bioleaching capability and efficiency of both strains;
- The MBM medium is more indicated than the R2A medium for bioleaching assays, once it allows the maintenance of an acid pH environment;
- *B. simplex* 10w-16b accumulates high quantities of W during the assays with wolframite (concentrated) as well as with Panasqueira mine tailings but it is not capable to mobilize the W to the medium;
- *C. cellasea* 10w-11 accumulates W during the assays with ore and with the mine tailings. Moreover, it is capable of bioleaching (mobilizing to the medium) W, as well as Cu and Zn, that exist in the Panasqueira mine tailings;
- Physical contact between the bacterial cells and the wolframite or the Panasqueira mine tailings is necessary to occur the bioaccumulation and the biomobilization of the metals to the environmental liquid (bioleaching processes).
- During bioleaching assays with lab-scale lysimeters the pH did not variate during the experiment, keeping the environment acid.

- Bioaugmentation and biostimulation of the Panasqueira mine tailing resulted in the mobilization of W at ppb level and mobilization of Se at ppm level.
- More bioleaching and molecular assays are needed to conclude about the microbiome role in metals mobilization to the culture medium during bioleaching assays with lab-scale lysimeters.

References

- ADAMS, G. O., FUFUYIN, P. T., OKORO, S. E., & EHINOMEN, I. (2015). Bioremediation, biostimulation and bioaugmentation: a review. *International Journal of Environmental Bioremediation & Biodegradation*, 3(1), 28-39.
- AGUILAR-BARAJAS, E., DÍAZ-PÉREZ, C., RAMÍREZ-DÍAZ, M. I., RIVEROS-ROSAS, H., & CERVANTES, C. (2011). Bacterial transport of sulfate, molybdate, and related oxyanions. *Biometals*, 24(4), 687-707.
- ALTSCHUL, S. F., GISH, W., MILLER, W., MYERS, E. W., & LIPMAN, D. J. (1990). Basic local alignment search tool. *Journal of molecular biology*, 215(3), 403-410.
- ANDREESEN, J. R., & MAKDESSI, K. (2008). Tungsten, the surprisingly positively acting heavy metal element for prokaryotes. *Annals of the New York Academy of Sciences*, 1125(1), 215-229.
- ANJUM, F., SHAHID, M., & AKCIL, A. (2012). Biohydrometallurgy techniques of low grade ores: A review on black shale. *Hydrometallurgy*, 117, 1-12.
- APPENROTH, K. J. (2010). Definition of “heavy metals” and their role in biological systems. In *Soil heavy metals* (pp. 19-29). Springer, Berlin, Heidelberg.
- AYANGBENRO, A. S., & BABALOLA, O. O. (2017). A new strategy for heavy metal polluted environments: a review of microbial biosorbents. *International journal of environmental research and public health*, 14(1), 94.
- BEVERS, L. E., HAGEDOORN, P. L., & HAGEN, W. R. (2009). The bioinorganic chemistry of tungsten. *Coordination Chemistry Reviews*, 253(3-4), 269-290.
- BRUINS, M. R., KAPIL, S., & OEHME, F. W. (2000). Microbial resistance to metals in the environment. *Ecotoxicology and environmental safety*, 45(3), 198-207.
- CHUNG, A. P., COIMBRA, C., FARIAS, P., FRANCISCO, R., BRANCO, R., SIMÃO, F. V., ... & MORTENSEN, M. S. (2019). Tailings microbial community profile and prediction of its functionality in basins of tungsten mine. *Scientific Reports*, 9(1), 1-13.
- COIMBRA, C., BRANCO, R., & MORAIS, P. V. (2019). Efficient bioaccumulation of tungsten by *Escherichia coli* cells expressing the *Sulfitobacter dubius* TupBCA system. *Systematic and applied microbiology*, 42(5), 126001.
- COIMBRA, C., FARIAS, P., BRANCO, R., & MORAIS, P. V. (2017). Tungsten accumulation by highly tolerant marine hydrothermal *Sulfitobacter dubius* strains carrying a tupBCA cluster. *Systematic and applied microbiology*, 40(6), 388-395.
- CORTEZ, H., PINGARRÓN, J., MUÑOZ, J. A., BALLESTER, A., BLÁZQUEZ, M. L., GONZÁLEZ, F., ... & COTO, O. (2010). 17. Bioremediation of soils contaminated with metalliferous mining wastes.
- CURTIN, J., & CORMICAN, M. (2003). Measuring antimicrobial activity against biofilm bacteria. *Reviews in Environmental Science and Biotechnology*, 2(2-4), 285-291.
- D'AMATO, D., DROSTE, N., ALLEN, B., KETTUNEN, M., LÄHTINEN, K., KORHONEN, J., LESKINEN, P., MATTHIES, B.D. & TOPPINEN, A. (2017). Green, circular, bio economy: A comparative analysis of sustainability avenues. *Journal of Cleaner Production*, 168, 716-734.

- DEVECI, H., AKCIL, A., & ALP, I. (2004). Bioleaching of complex zinc sulphides using mesophilic and thermophilic bacteria: comparative importance of pH and iron. *Hydrometallurgy*, 73(3-4), 293-303.
- DÍAZ, J. A., SERRANO, J., & LEIVA, E. (2018). Bioleaching of arsenic-bearing copper ores. *Minerals*, 8(5), 215.
- EGAN, J., BAZIN, C., & HODOUIN, D. (2016). Effect of particle size and grinding time on gold dissolution in cyanide solution. *Minerals*, 6(3), 68.
- FELLNER, J., LEDERER, J., SCHARFF, C., & LANER, D. (2017). Present potentials and limitations of a circular economy with respect to primary raw material demand. *Journal of Industrial Ecology*, 21(3), 494-496.
- GADD, G. M. (2010). Metals, minerals and microbes: geomicrobiology and bioremediation. *Microbiology*, 156(3), 609-643.
- GHOLAMIAN, S., GHOLAMIAN, S., NAZEMI, A., & NARGESI, M. M. (2013). Optimization of culture media for L-asparaginase production by newly isolated bacteria, *Bacillus* sp. GH5. *Microbiology*, 82(6), 856-863.
- GODINHO, B. R. C. (2009). Avaliação da qualidade ambiental da envolvente das Minas da Panasqueira. Vertente solo-água-Arbutus unedo. Um caso de estudo com orientação ambiental e social (Doctoral dissertation).
- GONÇALVES, A. C. R. (2012). Riscos associados à exploração mineira. O caso das minas da Panasqueira. *Cadernos de Geografia*, (30-31), 131-142.
- GRAENTZDOERFFER, A., RAUH, D., PICH, A., & ANDREESSEN, J. R. (2003). Molecular and biochemical characterization of two tungsten- and selenium-containing formate dehydrogenases from *Eubacterium acidaminophilum* that are associated with components of an iron-only hydrogenase. *Archives of microbiology*, 179(2), 116-130.
- GRATHWOHL, P. (2014). On equilibration of pore water in column leaching tests. *Waste management*, 34(5), 908-918.
- GROSSULE, V., & LAVAGNOLO, M. C. (2020). Lab tests on semi-aerobic landfilling of MSW under varying conditions of water availability and putrescible waste content. *Journal of Environmental Management*, 256, 109995.
- HAGEN, W. R. (2011). Cellular uptake of molybdenum and tungsten. *Coordination Chemistry Reviews*, 255(9-10), 1117-1128.
- HALL, T., BIOSCIENCES, I., & CARLSBAD, C. (2011). BioEdit: an important software for molecular biology. *GERF Bull Biosci*, 2(1), 60-61.
- HASSEN, A., SAIDI, N., CHERIF, M., & BOUDABOUS, A. (1998). Resistance of environmental bacteria to heavy metals. *Bioresource technology*, 64(1), 7-15.
- HUANG, D. W., SHERMAN, B. T., & LEMPICKI, R. A. (2009). Bioinformatics enrichment tools: paths toward the comprehensive functional analysis of large gene lists. *Nucleic acids research*, 37(1), 1-13.
- JOHNSON, M. K., REES, D. C., & ADAMS, M. W. (1996). Tungstoenzymes. *Chemical reviews*, 96(7), 2817-2840.
- JONES, P., & BOWN, R. (2020). Approaches to the Circular Economy. In *Handbook of Research on Contemporary Consumerism* (pp. 73-91). IGI Global.

- KANEHISA, M. (2002, JANUARY). The KEGG database. In Novartis Foundation Symposium (pp. 91-100). Chichester; New York; John Wiley; 1999.
- KRUGER, N. J. (2009). The Bradford method for protein quantitation. In *The protein protocols handbook* (pp. 17-24). Humana Press, Totowa, NJ.
- KUMAR, S., STECHER, G., & TAMURA, K. (2016). MEGA7: molecular evolutionary genetics analysis version 7.0 for bigger datasets. *Molecular biology and evolution*, 33(7), 1870-1874.
- LEONG, Y. K., & CHANG, J. S. (2020). Bioremediation of heavy metals using microalgae: Recent advances and mechanisms. *Bioresource technology*, 122886.
- LI, S., ZHONG, H., HU, Y., ZHAO, J., HE, Z., & GU, G. (2014). Bioleaching of a low-grade nickel–copper sulfide by mixture of four thermophiles. *Bioresource technology*, 153, 300-306.
- MARKOWITZ, V. M., CHEN, I. M. A., PALANIAPPAN, K., CHU, K., SZETO, E., GRECHKIN, Y., ... & HUNTEMANN, M. (2012). IMG: the integrated microbial genomes database and comparative analysis system. *Nucleic acids research*, 40(D1), D115-D122.
- MATHIEUX, F., ARDENTE, F., BOBBA, S., NUSS, P., BLENGINI, G. A., DIAS, P. A., ... & HAMOR, T. (2017). *Critical raw materials and the circular economy*. Publications Office of the European Union: Luxembourg.
- PAL, C., BENGTTSSON-PALME, J., RENSING, C., KRISTIANSSON, E., & LARSSON, D. J. (2014). BacMet: antibacterial biocide and metal resistance genes database. *Nucleic acids research*, 42(D1), D737-D743.
- PRESTA, L., FONDI, M., EMILIANI, G., & FANI, R. (2015). *Molybdenum Cofactors and Their Role in the Evolution of Metabolic Pathways*. Springer.
- RASOULNIA, P., BARTHEN, R., & LAKANIEMI, A. M. (2020). A critical review of bioleaching of rare earth elements: The mechanisms and effect of process parameters. *Critical Reviews in Environmental Science and Technology*, 1-50.
- SCHRÄDER, T., RIENHÖFER, A., & ANDREESEN, J. R. (1999). Selenium–containing xanthine dehydrogenase from *Eubacterium barkeri*. *European journal of biochemistry*, 264(3), 862-871.
- SIGEL, A., & SIGEL, H. (EDS.). (2002). *Metals ions in biological system: Volume 39: Molybdenum and tungsten: Their roles in biological processes*. CRC Press.
- TAYEBI-KHORAMI, M., EDRAKI, M., CORDER, G., & GOLEV, A. (2019). Re-Thinking Mining Waste through an Integrative Approach Led by Circular Economy Aspirations. *Minerals*, 9(5), 286.
- UNZ, R. F., & SHUTTLEWORTH, K. L. (1996). Microbial mobilization and immobilization of heavy metals. *Current Opinion in Biotechnology*, 7(3), 307-310.
- VALLS, M., & DE LORENZO, V. (2002). Exploiting the genetic and biochemical capacities of bacteria for the remediation of heavy metal pollution. *FEMS microbiology Reviews*, 26(4), 327-338.
- WANG, X., SUN, Z., LIU, Y., MIN, X., GUO, Y., LI, P., & ZHENG, Z. (2019). Effect of particle size on uranium bioleaching in column reactors from a low-grade uranium ore. *Bioresource technology*, 281, 66-71.
- WHITE, C., SAYER, J. A., & GADD, G. M. (1997). Microbial solubilization and immobilization of toxic metals: key biogeochemical processes for treatment of contamination. *FEMS microbiology reviews*, 20(3-4), 503-516.

WU, H., CAO, D., LIU, T., ZHAO, J., HU, X., & LI, N. (2015). Purification and characterization of recombinant human lysozyme from eggs of transgenic chickens. *PloS one*, 10(12).

Annexes

1. Culture media

1.1. Luria-Bertani (LB) medium

LB medium is a nutritionally rich medium and one of the most widely used medium for the growth of bacteria, especially for the growth of pure cultures. To 1 liter (L) with distilled water, 10 grams (g) of tryptone, 5g of yeast extract and 5g of sodium chloride (NaCl) were weighed and dissolved. Then, it was sterilized by autoclaving at 121 degrees Celsius (°C) for 20 minutes (min).

1.2. Mody-Bam-SM (MBM) medium

MBM is a modified medium through the combination of Mody and BAM mediums, supplemented with succinate and mannitol, being a very nutritionally rich medium. To a final volume of 1L, 10g of mannitol, 1g of glutamate, 0.5g of L-asparagine, 4g of succinate, 1g of ammonium nitrate (NH₄NO₃), 0.1 of sodium chloride (NaCl), 0.2g of magnesium sulfate heptahydrate (MgSO₄.7H₂O), 0.3g of monopotassium phosphate (KH₂PO₄) and 2g of yeast extract were weighed and dissolved in 800 milliliters (mL) of distilled water. The pH value was adjusted into 6.0 with hydrochloric acid (HCl) and then was adjusted with distilled water until 980mL. Then, it was sterilized by autoclaving at 121 °C for 20 min. After the sterilization process, 20mL of Glucose 50% was added to the culture medium.

1.3. Reasoner's 2A broth (R2A) medium

R2A broth medium (HiMedia), a low nutrient medium, is used for the cultivation and maintenance of heterotrophic bacteria from potable waters. To 1L, 3.12g of the

powder was weighed and dissolved with distilled water. Then, it was sterilized by autoclaving at 121 °C for 20 min.

2. Solutions and Reagents

2.1. Stock solution of Glucose 50%

50g of glucose was weighed and dissolved with 100mL of distilled water, and then sterilized by autoclaving at 121 °C for 20 min.

2.2. Stock solution of molybdenum, 1 Molar (M)

4.8g of Sodium Molybdate ($\text{Na}_2\text{MO}_4 \cdot 2\text{H}_2\text{O}$) (BDH) was weighed and dissolved with 50mL of distilled water and sterilized by filtration with a filter of 0.2 micrometers (μm).

2.3. Stock solution of tungsten, 1M

9.2g of sodium tungstate dehydrate ($\text{Na}_2 \cdot \text{WO}_4 \cdot 2\text{H}_2\text{O}$) (Sigma-Aldrich) was weighed and dissolved with 50mL of distilled water and sterilized by filtration with a filter of 0.2 μm .

2.4. Nitric Acid (HNO_3) solution 10%

10mL of HNO_3 was dissolved with 90mL of distilled water.

2.5. Lysozyme solution

10 milligram (mg) of lysozyme was weighed and dissolved in 1mL of sterile water.

2.6. Phosphate Buffered Solution (PBS) solution

To 1L, 80g of NaCl, 2g of potassium chloride (KCl), 14.4g of disodium phosphate (Na_2HPO_4) and 2.4g of monopotassium sulfate (KH_2PO_4) was weighed and dissolved in 800mL of distilled water. The pH value was adjusted to 7.4 with hydrochloric acid (HCl) and then was adjusted with distilled water until 1L. The PBS solution was stored at room temperature.

2.7. 1.5M Tris-HCl, pH 8.8

18.2g of Tris was weighed and dissolved in 60mL of distilled water. The pH value was adjusted to 8.8 using HCl, and then the volume was adjust to 100mL. The solution was stored at -4°C .

2.8. 0.5M Tris-HCl, pH 6.8

6g of Tris was weighed and dissolved in 60mL of distilled water. The pH value was adjusted to 6.8 using HCl, and then the volume was adjust to 100mL. The solution was stored at -4°C .

2.9. Dye solution

2.5g of Coomassie Brilliant Blue R was weighed and dissolved in 450mL of distilled water, as well as 454mL of Methanol and 96mL of Glacial Acetic Acid. The volume was adjusted to 1L. The dye solution was stored at room temperature.

2.10. Bleach solution

250ml of Methanol and 75ml Glacial Acetic Acid was added to 675mL of distilled water. The dye solution was stored at room temperature.

2.11. Stock solution of Tris-acetate (TAE) 50x

Add 121g of Tris Base, 50mL of EDTA, 0.5M and pH8.0, and 28.55mL of Glacial Acetic Acid. Adjust the pH to 8.0 using sodium hydroxide (NaOH), 5M and then add distilled water until 500mL. Store the solution at room temperature in a dark bottle.

2.12. TAE 1x

Dilute the previous solution in distilled water (1:50 - 1mL TAE 50x in 49mL distilled water).

2.13. Stock solution of Electrode (Running) Buffer 5x (SDS-PAGE)

Add 15.15g of Tris and 72g of Glycine to 800mL of distilled water. Adjust the pH to 8.8 and add distilled water until 1L.

2.14. Electrode Buffer 1x

Dilute 200mL of the stock solution (5x) with 800mL of distilled water, for each run.

3. Agarose gel 1% weight/volume (w/v)

1g of agarose was weighed into a 250 Erlenmeyer flask. Then, it was added 100mL of TAE 1x solution into the respective e Erlenmeyer flask and was swirled to mix. This solution was heated in a microwave for about 3 or 4 minutes to dissolve the agarose (the flask was shaken several times to promote and facilitate the dissolution of the agarose) and was left to cool at room temperature, stirring occasionally for 5 min. During the processes of heating and cooling, the electrophoresis equipment was prepared, putting

the combs. After cooling, the ethidium bromide (12 μ L) was added to the mixture and was stirred to mix.

The gel was placed carefully into the tank and all the formed bubbles were removed using the combs. Then, the gel was left to polymerize, and after that, before use, the combs were slowly removed from the gel.